Bull. Southern California Acad. Sci.
120(2), 2021, pp. 49–58
© Southern California Academy of Sciences, 2021

Mammal Activity and Species Richness is Reduced in Areas with Recreationists, in Palos Verdes Peninsula Habitat Fragments

Austin L. Nash

Department of Ecology and Evolutionary Biology, University of Colorado, Boulder, CO, austin.nash@colorado.edu

Abstract.—This study examined how the species richness and activity patterns of mammals differed in previously unsurveyed habitat fragments with varying recreation intensities on the Palos Verdes Peninsula, Los Angeles County, California. I hypothesized that the number of mammal species detected and activity level of mammals was reduced in habitat fragments with recreation present. Eight game cameras were installed in two habitat fragments in the Palos Verdes Peninsula (PVP), one canyon with recreation (hiking, biking, dog walking) and one reference canyon with minimal human use. Cameras were placed at natural constrictions along the two main travel corridors in the canyons, trails and creek beds. The camera installations were monitored for 200 d. Species richness, activity location, and activity time were analyzed for each canyon. The reference canyon had a higher number of mammal species detected (nine versus six) and accounted for 93% of wildlife detections. *Canis latrans* showed no difference in the number of detections between canyons, while the other eight mammal species detected exhibited higher activity in the reference canyon. *Canis latrans* exhibited greater variability in time of activity in the reference canyon than conspecifics in the recreation canyon. Mesopredators *Procyon lotor* and *Felis catus* accounted for 67% of wildlife detections in the canyon free of recreation and pose a potential risk to songbirds of conservation concern present in the PVP. Although limited by sampling constraints, this study provides a foundation to investigate wildlife dynamics in the network of habitat fragments in the Palos Verdes Peninsula.

As the human population continues to grow, urban development is reducing available habitat for wildlife (George and Crooks 2006). Los Angeles County, California, USA, is one location where a growing urban area is encroaching into natural landscapes. Due to the proximity of residential developments and natural open spaces, many people access wildlife habitat in and around Los Angeles County. Thus, Los Angeles County is an ideal place to study the effects of urbanization and human presence on wildlife species (Tigas et al. 2002; Ordenana et al. 2010; George and Crooks 2006; Riley et al. 2003; Benson, Sikich and Riley 2016; Ng et al 2003). The Palos Verdes Peninsula (PVP), a coastal landform southwest of the center of the city of Los Angeles, provides a unique opportunity to augment previous studies of the urban wildlife of the Los Angeles area (Riley et al. 2003; Ng et al. 2004; Ordeñana 2010), as the mammal species present have not been surveyed and their activity patterns in relation to humans have not been studied. Sage scrub canyons with varying levels of human recreation in PVP are a natural experimental system to study effects of recreation on wildlife habitat within an urban matrix.

Many non-consumptive recreationists believe they have little to no impact on wildlife species, but several studies indicate that this assumption is incorrect (Larson et al. 2016; Taylor and Knight 2003). Recreational disturbances, such as trail creation and use, can cause harm to wildlife by direct mortality, habitat alteration, or by altering wildlife be-

Downloaded from http://meridian.allenpress.com/scasbulletin/article-pdf/120/2/49/2930757/i2162-4534-120-2-49.pdf by guest on 12 December 2024

haviors (Kays et al. 2017; Reilly et al. 2017). Outdoor recreation in these habitat areas places humans and wildlife in a space where interaction is possible, altering the behavior of wildlife, changing the temporal and spatial distribution of mammals and putting recreationists at risk of harm (Benson et al. 2016; Kays et al. 2017). For example, coyotes restrict activity times in areas with high recreation (George and Crooks 2006; Benson et al., 2016) and the presence of dogs along trails reduces small mammal activity (Lenth et al. 2008). Recreational trails in habitat fragments throughout the PVP are used by hikers, dog-walkers and mountain bikers in addition to wildlife and provide opportunities for interactions. Land managers of the PVP and other urban habitat fragments can create better informed management plans if the impacts of recreationists on mammal wildlife species, such as temporal and spatial alterations in wildlife behavior, are known (Larson et al. 2016; Riley et al. 2016; Kays et al. 2017).

Additionally, interactions between humans and wildlife can lead to conflict that puts humans and wildlife at risk of harm (White and Gehrt 2009). Los Angeles County has one of the highest sympatric populations of humans and coyotes in the United States (Elliot et al. 2016). The coyote (*Canis latrans*) is the largest bodied mammalian predator on the PVP, making it a key urban focal study species to determine risk of conflict and is of concern to PVP residents (White and Gehrt 2009; Ordeñana 2010; pers. obs.). Wildlife and recreationists must be both present in the same place and time for a conflict instance to occur. However, some wildlife species, such as coyotes, have adapted well to urban areas through behavioral shifts towards nocturnality, while most recreation occurs diurnally, possibly limiting interactions (Grinder and Krausman 2015; Gehrt 2011; Ordeñana 2010).

This study aims to identify which mammal species are present in two habitat fragments in PVP, assess how mammal community activity and species richness are potentially affected by human recreation, and evaluate the possibility of interactions between mammal wildlife species and recreationists. I addressed these questions by placing game cameras in protected PVP canyons of sage scrub habitat fragments of similar size, shape, and isolation, but with or without recreation. I hypothesized that (I) canyons with recreation will have a reduced number of mammal species detected compared to those without, (II) canyons with recreation will have reduced mammal species activity measured by detection rate, (III) mammals in the recreation canyons will display more nocturnal activity while recreationists will be present during the day. The goal of this study is to inform natural resource managers of the PVP of Los Angeles, California and provide baseline information to initiate more complex studies of wildlife in urban matrices using the PVP.

Materials and Methods

Mammalian responses to recreation were studied in two undeveloped canyons surrounded by suburban development (Margate and Agua Amarga Canyon), situated in the PVP, a coastal suburban landform located in the southwest corner of Los Angeles County, CA USA (Fig. 1). Both Margate and Agua Amarga Canyons have steep hillsides with a dry creek bed running the length of each canyon from west to east. Margate and Agua Amarga canyon are separated by two km and are located on the western side of the PVP (Fig. 1). The dominant plant species in both canyons include native chapparal plants such as lemonadeberry, *Rhus integrifolia* and California sagebrush, *Artemisia californica*, in addition to the invasive common fennel, *Foeniculum vulgare*, and black mustard, *Brassica nigra*. Human presence in Margate Canyon is limited to a municipal services access trail. Agua Amarga Canyon, however, has an established trail for recreation running parallel to

Downloaded from http://meridian.allenpress.com/scasbulletin/article-pdf/120/2/49/2930757/i2162-4534-120-2-49.pdf by guest on 12 December 2024

Fig. 1. Camera locations in the reference and recreation canyons in relation to the PVP. (NAIP Aerial Imagery)

the creek bed on one side of the canyon and experiences high levels of hiking, bicycling and walking of domestic dogs, *Canis familiaris*. These similar canyons serve as effective sites to study the effects of recreation within urban fragments on the behavioral ecology of mammals due to the disparity in human activity between canyons. The Palos Verdes Peninsula itself is an excellent system for studying urban wildlife in open space surrounded by urban

Downloaded from http://meridian.allenpress.com/scasbulletin/article-pdf/120/2/49/2930757/i2162-4534-120-2-49.pdf by guest on 12 December 2024

matrix as it has over 25 open space areas of varying visitor-use levels, size, and isolation that are all separated from any large contiguous areas of habitat by the heavy development of the Los Angeles metropolitan area.

Game cameras (Bushnell Model #119537, Overland Park, Kansas, USA) were installed in pairs along a perpendicular axis of both canyon's length with one camera in the creek bed and one camera on the trail to monitor mammal and recreation usage. One camera pair was located near the western mouth of both canyons and another pair was located further east in both canyons relatively near a point of access, for a total of 8 camera installations between the two canyons. Given camera limitations, subsampling the two canyons with four cameras for within-site replication was chosen over more canyons with lower within-site replication, reducing the importance of the placement of an individual camera within the canyons.

Cameras were installed at (33.767418, -118.407337 Agua Amarga Western Creek), (33.766818, -118.406139 Agua Amarga Western Trail), (33.767926, -118.400342 Agua Amarga Eastern Creek), (33.767579, -118.400528 Agua Amarga Eastern Trail), (33.785458, -118.409238 Margate Eastern Creek), (33.785237, -118.408921 Margate Eastern Trail), (33.785000, -118.411250 Margate Western Creek), and (33.784798, -118.411085 Margate Western Trail). Camera locations were selected at natural constrictions in the canyons to reduce the ability of mammals to travel past the camera without being detected and were placed in areas with vegetation communities representative of the canyon in which they were placed. Cameras were angled downwards and along the length of the travel path to minimize the recording of public visitors' faces while maximizing mammal and recreationist detections. Placing game cameras along trails instead of random placement has been shown to not affect community richness or composition conclusions given sufficient sampling effort (more than 1400 trap nights) (Cusack 2015). Cameras in this study were deployed for 1503 camera trap nights (i.e., 24-hr periods per camera). Cameras were deployed from 3 May 2017 to 18 November 2017. This project was permitted through the City of Palos Verdes Estates (permit number 023252) and given permission to proceed by the Palos Verdes Peninsula Land Conservancy when on Conservancy land.

Cameras were set to record a 30 sec video per motion detected trigger with a delay of 10 sec between triggers. Batteries and SD cards were replaced biweekly, and videos were manually sorted as mammal detections, recreation detections (human or domestic dog) or no detection. A detection was categorized as at least one mammal in frame; mammals were not double counted if they left and re-entered the frame in the same video, and multiple individuals in the same video counted as multiple detections. The same protocol was used for scoring recreation detections. The number of detections per species at each camera location was recorded for each biweekly period, as day (color images) or night (infrared images). This ensured that the cutoff between day and night was as consistent as possible throughout changing seasons. Additionally, this method may be more effective than using time to designate night and day for studies utilizing game cameras through multiple seasons as it is reliant on the intensity of light itself.

Detections from the western and eastern cameras for creek bed and trail were combined by canyon in the analysis to reduce the effect of individual camera placement within each canyon. For example, data from the Margate western and eastern creek bed cameras were combined to create reference creek bed in the final dataset. Additionally, for some analyses data from all cameras in each canyon were combined to create the recreation and reference categories. To control for uneven sampling between sites due to camera failures, I used the minimum number of trap days without failures, 161 d to scale the data from

Downloaded from http://meridian.allenpress.com/scasbulletin/article-pdf/120/2/49/2930757/i2162-4534-120-2-49.pdf by guest on 12 December 2024

each camera. Average trap days per camera was 188 trap d with a standard deviation of 15 d.

I compared the total number of dog and human detections ('recreation') between the two canyons and the number of total wildlife detections between canyons using a Chi-square test ($\alpha = 0.05$) as detections were independent, mutually exclusive counts. I compared the proportion of detections that were nocturnal between the recreation and reference canyons using a t-test ($\alpha = 0.05$). I compared the mammal average species richness for every two-week segment (each camera deployment) of the full data collection period between the two canyons using a t-test ($\alpha = 0.05$).

Results

I recorded 652 detections of mammalian wildlife species and 8,117 detections of domestic dogs and humans between both canyons. Only 29 human photos were recorded over a 200-d period in the reference canyon, while a total of 8,088 human and domestic dog detections were recorded in the recreation canyon, demonstrating the canyons were effective treatments for recreation ($\chi^2 = 8001$, $p < 0.01$). The high number of dog detections, 5116, in the recreation canyon is partially due to one dog walker who walked 8-12 dogs past the Agua Amarga Western Creek bed camera multiple times per week.

The reference canyon had a total species richness count of 9 species and mean of 2.46 species observed per two-wk period. The recreation canyon had 6 species total and a mean of 0.54 species detected per two-wk period. There was a lower species richness per two-wk data collection period in the recreation canyon ($t = 5.69$, $p < 0.01$). Species observed in all sites were coyote (*Canis latrans*), feral cat (*Felis catus*), raccoon (*Procyon lotor*), desert cottontail rabbit, (*Sylvilagus audubonii),* striped skunk (*Mephitis mephitis*), and fox squirrel (*Sciurus niger*) (Fig. 1). Mammals detected in only the reference canyon were the Virginia opossum (*Didelphis virginiana*), black rat (*Rattus rattus*), and red fox (*Vulpes vulpes*). There were no species detected only in the recreation canyon. Two mesopredators, raccoons and feral cats accounted for the majority of detections (41% and 26%, respectively). Black rat was the third most detected species (12%), followed by desert cottontail (7%), striped skunk (5%), opossum (4%), fox squirrel (3%), coyote (1%), and red fox (1%).

The number of mammal detections was 13.5 times greater in the reference canyon as compared to the recreation canyon. Coyotes were observed in both canyons with no significant difference in activity between the two canyons, ($\chi^2 = 0.14$, $p = 0.71$). All other mammal species displayed higher activity in the reference canyon ($p < 0.05$; Table 1). Raccoon and striped skunks showed the greatest difference in activity between canyons, with 28 and 31 times more detections in the reference canyon, respectively. Nocturnal mammal activity occurred much more frequently than diurnal activity overall, ($\chi^2 = 271.42$, $p < 0.01$; Table 1) with 537 nocturnal mammal detections compared to 116 mammal detections during the day. Black rat, Virginia opossum, red fox and striped skunk were only detected at night. Fox squirrel was the only strictly diurnal mammal. Raccoon detections occurred at night except for four daytime detections in the reference canyon and were thus more nocturnal (reference canyon: $\chi^2 = 187.32$, $p < 0.01$) and (recreation: $\chi^2 = 8.00$ $p < 0.01$). Feral cats were detected at night more often than during the day in both canyons, (recreation: $\chi^2 = 14.22$, $p < 0.01$) and (reference: $\chi^2 = 10.8$, $p < 0.01$). For desert cottontail rabbit, diurnal activity was more frequent in the reference canyon ($\chi^2 = 11.57$, $p < 0.01$), while in the recreation canyon there was no significant difference in time of activity ($\chi^2 = 0.66$, $p = 0.41$). Coyotes displayed greater nocturnal activity in the recreation but not in the reference canyon, ($\chi^2 = 4.00$, $p = 0.045$ and $\chi^2 = 0.33$, $p = 0.56$ respectively).

Downloaded from http://meridian.allenpress.com/scasbulletin/article-pdf/120/2/49/2930757/i2162-4534-120-2-49.pdf by guest on 12 December 2024

Downloaded from http://meridian.allenpress.com/scasbulletin/article-pdf/120/2/49/2930757/i2162-4534-120-2-49.pdf by guest on 12 December 2024

Table 1. Results of Chi-Squared Analyses of activity between canyons, between trail types in each canyon, and between day and night in each canyon.

	Total Detections				*Detections by Activity Time*							
Species	Reference Canyon	Recreation Canyon	CHI-SQ	p-value	Reference Night	Reference Day	CHI-SQ	p-value	Recreation Night	Recreation Day	CHI-SQ	p-value
Procyon lotor	203	8	180.21	4.35E-41	199	4	187.32	1.23E-42	8	0	8	4.68E-03
Felis catus	120	18	75.39	3.86E-18	78	42	10.8	1.02E-03	17	1	14.22	1.62E-04
Rattus rattus	61	0	61	5.71E-15	61	0	61	5.71E-15	0	0	-	-
Sylvilagus audubonii	28	6	14.24	1.61E-04	5	23	11.57	6.70E-04	2	4	0.66	0.41422
Mephitis mephitis	25	1	22.15	2.52E-06	25	0	25	5.73E-07	1	0	1	0.31731
Didelphis virginiana	20	0	20	7.74E-06	20	0	20	7.74E-06	0	0	-	-
Sciurus niger	15	3	8	4.68E-03	0	15	25	1.08E-04	0	3	3	0.08326
Canis latrans	3	4	0.14	0.705	2	1	0.33	0.5637	4	0	4	0.0455
Vulpes vulpes	4	0	4	4.55E-02	4	0	4	4.55E-02	0	0	-	-

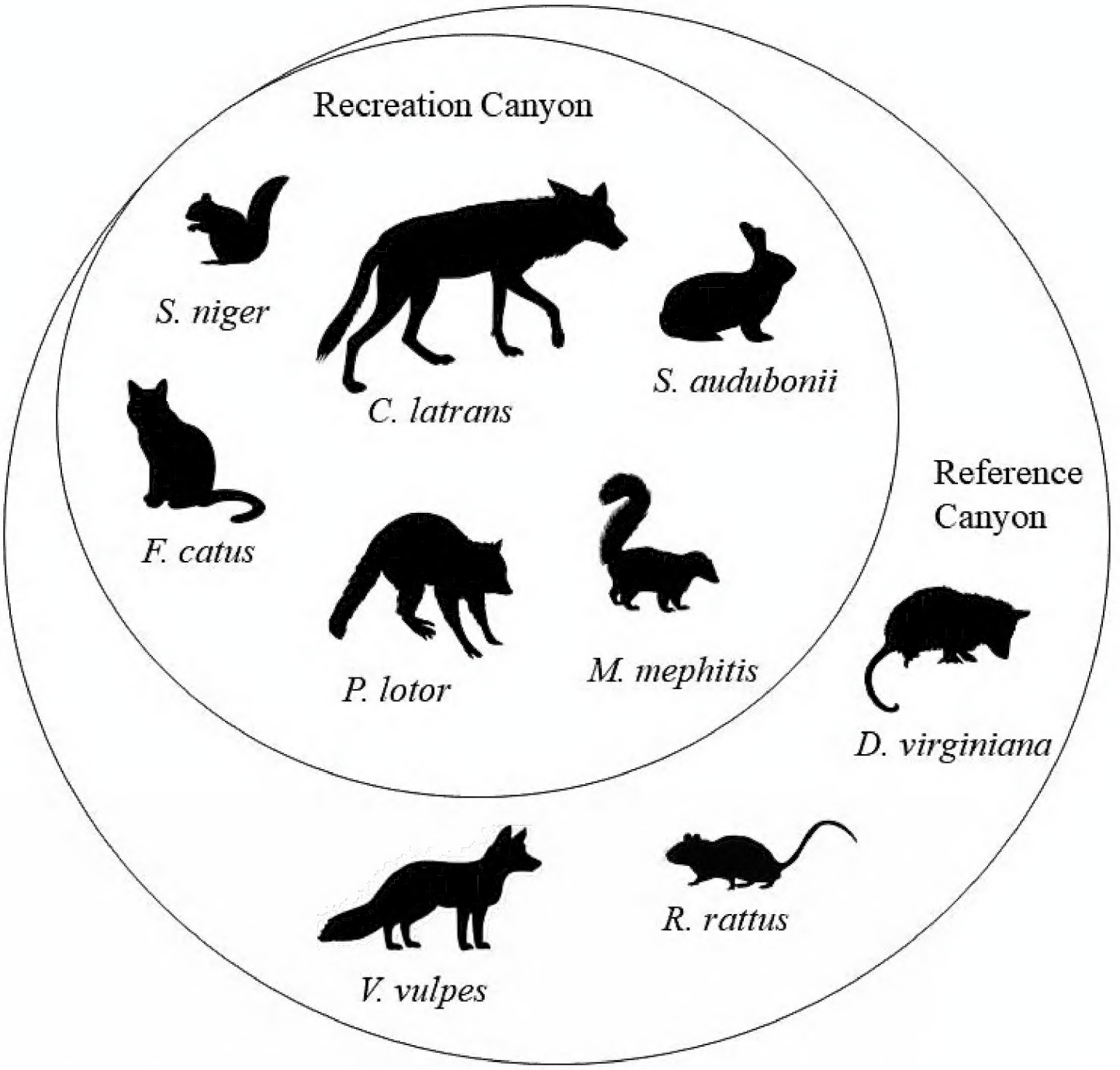

Fig. 2. Mammal species richness was reduced from nine to six species in the recreation canyon. The mammal community in the recreation canyon was a subset of the reference canyon community.

The only daytime detection of a coyote occurred along the trail in the reference canyon. The only non-solitary coyotes detected were a pair in the recreation canyon along the trail at night. Overall, 99.5% of all recreationist activity occurred during the day while 82% of mammal detections occurred at night. Between the two canyons, there was no difference in the proportion of all mammal detections that occurred at night ($t = 0.12$, $p = 0.906$).

Discussion

As human development continues to encroach on natural open spaces, human recreation demand and the habitat needs of wildlife will continue to overlap, necessitating knowledge on how to reduce wildlife-recreationist conflict. I detected reduced mammal activity and fewer mammal species where recreation was prevalent, building upon previous similar findings in other regions (Fig. 2; Tucker et al. 2018; Larson et al. 2016). There was 13.5 times the amount of mammal activity in the reference canyon, suggesting a reduction of animal activity due to human presence, a trend found in a global meta-analysis across 57 mammal species (Tucker 2018). Reductions in activity due to human presence could reduce the like-

Downloaded from http://meridian.allenpress.com/scasbulletin/article-pdf/120/2/49/2930757/i2162-4534-120-2-49.pdf by guest on 12 December 2024

lihood of animals moving between fragments, possibly leading to reduced genetic diversity in these small remnant populations (Tucker 2018). Untangling whether this reduction in activity is due to reduced population sizes or reduced levels of individual activity is warranted for future investigation.

The mammal species I detected were a relatively even combination of native and non-native species, representing a novel mammal assemblage. For example, while the gray fox, *Urocyon cinereoargenteus* is native to Southern California and present in other nature preserves in the PVP the non-native red fox was present in both study canyons. Red foxes could fill the same functional role as gray foxes or lead to novel biotic interactions. Uncertain ecological consequences make determining the conservation outlook for these novel assemblages challenging (Kowarik 2011). Furthermore, these novel mammal assemblages can alter remaining native vegetation and wildlife communities in these habitat fragments (Chase 2006).

Raccoons and feral cats represented 67% of wildlife detections in the reference canyon and had higher activity in the reference canyon compared to the recreation canyon. Feral cat populations are especially concerning as they have been shown to be effective predators of species of conservation concern (Fitzgerald 1979; Chase 2006). In Agua Amarga Canyon, the possible increase in feral cat predation could be harmful to local populations of cactus wren, *Campylorhynchus brunneicapillus*, a species of local conservation concern (Dalkey 2016) and California gnatcatcher, *Polioptila californica*, a federally threatened species and California species of special concern (CDFW 2020). Thus, mesopredators are contributing the majority of detections in these canyons and are an important group to understand to better manage urban preserves for native songbird persistence (Crooks 2002; Crooks and Soulé 1999; Cove et al. 2014).

Wildlife diel activity patterns did not differ significantly from expected patterns for each species and detections were dominated by nocturnal and crepuscular species. Thus, serious human-wildlife conflict seems unlikely in the study canyons, as 82% of wildlife detections occurred at night while 99.5% of recreationist detections occurred during the day and 98% of wildlife detections were either raccoons or a species of smaller body size (Fig. 3).

This study utilized the natural exclusion of human recreation in the reference canyon to investigate how recreation affects the species richness and activity patterns of mammals. I acknowledge strong limitations to this preliminary study due to limited resources. Thus, the sample size of two canyons and eight cameras limits the generalizability of these results to urban wildlife and recreation generally. Sampling many areas with a gradient of human activity would reduce the likelihood that observed effects were due to some intrinsic characteristic of the canyon as opposed to human activity level. Other differences between the two canyons that could be alternative drivers of the observed patterns in mammal species and activity detected include active habitat restoration work in the recreation canyon and the slightly larger size of the recreation canyon. Longer sampling periods allowing for stronger analyses at the species level would reduce the dominating effect of the high number of feral cat and raccoon detections. Given these limitations, my conclusions are preliminary but consistent with previous findings on reduced species richness (Larson et al. 2016) and activity (Tucker et al. 2018) from human activity. Lastly, this study represents the first published study of urban wildlife in the PVP and there is significant possibility for very robust studies of urban wildlife using PVP open space areas.

Palos Verdes Peninsula has strong potential to serve as a study system for wildlife in open space, as there are more than 25 open space areas of varying size and isolation. Sampling many open space areas and utilizing techniques such as occupancy modeling to account

Downloaded from http://meridian.allenpress.com/scasbulletin/article-pdf/120/2/49/2930757/i2162-4534-120-2-49.pdf by guest on 12 December 2024

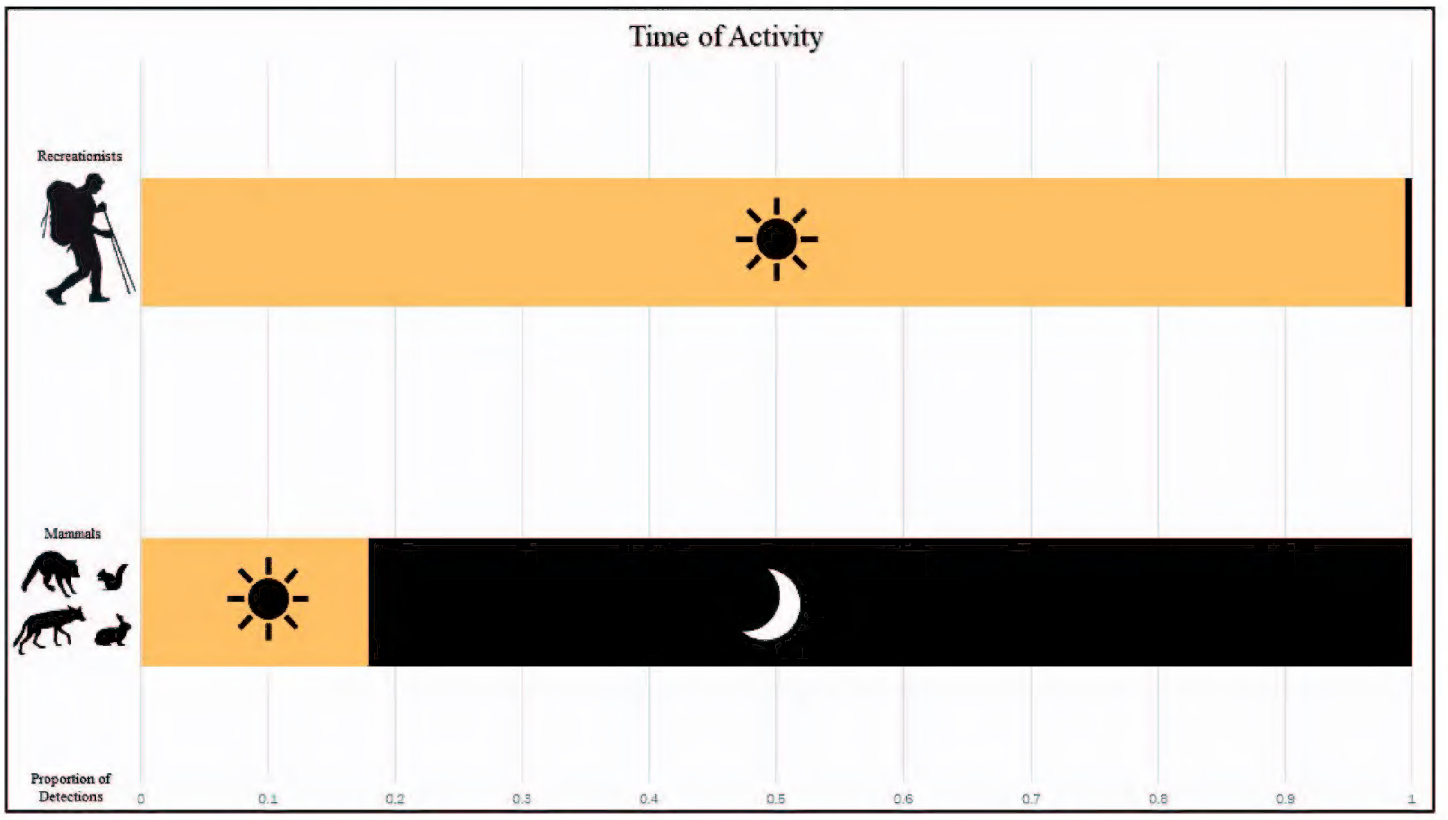

Fig. 3. Total proportion of detections of recreationists and of wildlife occurring at day and night. 99.5% of all recreationist activity occurred during the day while 82% of mammal detections occurred at night.

for imperfect detection (Mackenzie et al. 2002) would improve the strength of inference of future related studies. Questions that should be investigated in PVP preserves include how wildlife use areas with and without recreation within the same urban preserve and if they travel between reserves to avoid human activity (Atwood et al. 2016), to better understand how to reduce impact on mammal species without excluding recreationists from the last open spaces left in the PVP.

Conclusions

Mammal species richness and activity were reduced in a canyon with recreation as compared to a canyon without recreational activity in the PVP. The mammal communities of both canyons represent a novel assemblage of both native and non-native mammals. Mesopredators were by far the most detected group of mammals, which is concerning given the presence of two songbirds of conservation concern in the PVP. This preliminary study is limited by sampling constraints but is consistent with previous findings on urban wildlife responses to human recreation. The PVP, a matrix of habitat fragments and development isolated from large protected natural areas, provides a suitable system for understanding how wildlife persist within an urban-habitat matrix.

Acknowledgments

Dr. Theodore Stankowich and Rita Collins provided equipment. Tommy Jankowski and Brandon Nash provided support as field assistants. Dr. Travis Gallo and Dr. Christy McCain were both important help with the manuscript. I recognize the Palos Verdes Peninsula Land Conservancy for allowing me to place cameras on Conservancy land.

Literature Cited

Atwood, T.C., Weeks, H.P., and Gehring, T.M. 2004. Spatial ecology of coyotes along a suburban-to-rural gradient. J. Wildl. Manag., 68:1000-1009.

Downloaded from http://meridian.allenpress.com/scasbulletin/article-pdf/120/2/49/2930757/i2162-4534-120-2-49.pdf by guest on 12 December 2024

Benson, J.F., Sikich, J.A., and Riley, S.P. 2016. Individual and population level resource selection patterns of mountain lions preying on mule deer along an urban-wildland gradient. PLOS One, 11:e0158006.

Chace, J.F., and Walsh, J.J. 2006. Urban effects on native avifauna: a review. Landsc. Urban Plan., 74:46-69.

Cove, M.V., Spínola, R.M., Jackson, V.L., and Saénz, J.C. 2014. The role of fragmentation and landscape changes in the ecological release of common nest predators in the Neotropics. PeerJ, 2:e464.

Crooks, K.R. 2002. Relative sensitivities of mammalian carnivores to habitat fragmentation. Conserv. Biol., 16:488-502.

Crooks, K.R., and Soulé, M.E. 1999. Mesopredator release and avifaunal extinctions in a fragmented system. Nature, 400:563.

Cusack, J.J., Dickman, A.J., Rowcliffe, J.M., Carbone, C., Macdonald, D.W., and Coulson, T. 2015. Random versus game trail-based camera trap placement strategy for monitoring terrestrial mammal communities. PLOS One, 10:e0126373.

Dalkey, A. 2016. Site fidelity of a coastal cactus wren (*Camphylorynchus brunneicapillus*) on the Palos Verdes Peninsula. BSCAS, 115:141-146.

Elliot, E.E., Vallance, S., and Molles, L.E. 2016. Coexisting with coyotes (*Canis latrans*) in an urban environment. Urban Ecosyst., 19:1335-1350.

Fitzgerald, B.M., and Karl, B.J. 1986. Home range of feral house cats (*Felis catus L.*) in forest of the Orongorongo Valley, Wellington, New Zealand. N. Z. J. Ecol., 9:71-82.

Gehrt, S.D., Brown, J.L., and Anchor, C. 2011. Is the urban coyote a misanthropic synanthrope? The case from Chicago. C.A.T.E., 4:3.

George, S.L., and Crooks, K.R. 2006. Recreation and large mammal activity in an urban nature reserve. Biol. Conserv., 133:107-117.

Grinder, M.I., and Krausman, P.R. 2001. Home range, habitat use, and nocturnal activity of coyotes in an urban environment. J. Wildl. Manag.,, 887-898.

Kays, R., Parsons, A.W., Baker, M.C., Kalies, E.L., Forrester, T., Costello, R., Rota, C.T., Millspaugh, J.J. and McShea, W.J., 2017. Does hunting or hiking affect wildlife communities in protected areas? J. Appl. Ecol., 54:242-252.

Kowarik, I. (2011). Novel urban ecosystems, biodiversity, and conservation. Environ. Pollut., 159(8-9), 1974-1983.

Larson, C.L., Reed, S.E., Merenlender, A.M., and Crooks, K.R. 2016. Effects of recreation on animals revealed as widespread through a global systematic review. PLOS One, 11:e0167259.

Lenth, B.E., Knight, R.L., and Brennan, M.E. 2008. The effects of dogs on wildlife communities. Nat. Areas J., 28:218-228.

MacKenzie, D.I., Nichols, J.D., Lachman, G.B., Droege, S., Andrew-Royle, J., and Langtimm, C.A. (2002). Estimating site occupancy rates when detection probabilities are less than one. Ecology, 83(8), 2248-2255.

Ng, S.J., Dole, J.W., Sauvajot, R.M., Riley, S.P., and Valone, T.J. 2004. Use of highway undercrossings by wildlife in southern California. Biol. Conserv., 115:499-507.

Ordeñana, M.A., Crooks, K.R., Boydston, E.E., Fisher, R.N., Lyren, L.M., Siudyla, S., Haas, C.D., Harris, S., Hathaway, S.A., Turschak, G.M. and Miles, A.K., 2010. Effects of urbanization on carnivore species distribution and richness. J. of Mammal., 91(6):1322-1331.

Reilly, M.L., Tobler, M.W., Sonderegger, D.L., and Beier, P. 2017. Spatial and temporal response of wildlife to recreational activities in the San Francisco Bay ecoregion. Biol. Conserv., 207:117-126.

Riley, S.P., Sauvajot, R.M., Fuller, T.K., York, E.C., Kamradt, D.A., Bromley, C., and Wayne, R.K. 2003. Effects of urbanization and habitat fragmentation on bobcats and coyotes in southern California. Conserv. Biol., 17:566-576.

Taylor, A.R., and Knight, R.L. 2003. Wildlife responses to recreation and associated visitor perceptions. Ecol. Appl., 13:951-963.

Tigas, L.A., Van Vuren, D.H., and Sauvajot, R.M. 2002. Behavioral responses of bobcats and coyotes to habitat fragmentation and corridors in an urban environment. Biol. Conserv., 108:299-306.

Tucker, M.A., Böhning-Gaese, K., Fagan, W.F., Fryxell, J.M., Van Moorter, B., Alberts, S. C., et al. and Bartlam-Brooks, H. 2018. Moving in the Anthropocene: Global reductions in terrestrial mammalian movements. Science, 359:466-469.

White, L.A., and Gehrt, S.D. 2009. Coyote attacks on humans in the United States and Canada. Hum. Dimens. Wildl., 14:419-432.

Downloaded from http://meridian.allenpress.com/scasbulletin/article-pdf/120/2/49/2930757/i2162-4534-120-2-49.pdf by guest on 12 December 2024

Bull. Southern California Acad. Sci.
120(2), 2021, pp. 59–63
© Southern California Academy of Sciences, 2021

Sightings of a White Shark (*Carcharodon carcharias*) with a Significantly Deformed Pectoral Fin off the coast of Southern California

Phillip C. Sternes[1]* and Patrick L. Jambura[2]

[1]*Department of Evolution, Ecology, and Organismal Biology, University of California, Riverside, CA 92521*
[2]*Department of Paleontology, University of Vienna, Austria*

It is well known that sharks frequently suffer injuries throughout their life due to various natural causes (Pratt and Carrier 2001; Chin et al. 2015; Becerril-García et al. 2020), including human interactions (Lester et al. 2020). Although sharks show both remarkable resilience and wound-healing capabilities (Reif 1978; Womersely et al. 2021) to minor injuries such as lacerations, some injuries are so substantial that they remain present for the rest of the individual's life (Mumby 2019; Womersely et al. 2021). For example, in 2014 a grey reef shark, *Carcharhinus amblyrhynchos* (Bleeker, 1856), was observed to be missing its entire first dorsal fin at a reef near Palau (Mumby 2019). Remarkably, the same individual was seen again four years later near the original study site, indicating that it had survived with the permanent injury (Mumby 2019). It is known that the dorsal fin either aids in stability or in generating thrust depending on its size and position on the body (Lingham-Soliar 2005; Maia et al. 2017). However, it is unknown what functional consequences a shark may suffer when missing a dorsal fin (Harris 1936). Nevertheless, it was concluded that this grey shark most likely used a variety of feeding tactics to capture prey and survive to compensate the loss of its dorsal fin (Mumby 2019). Whereas grey reef sharks are moderately sized mesopredators (Roff et al. 2016), it is unknown how such injuries may impact the behavior and survival of large predatory sharks such as the white shark, *Carcharodon carcharias* (Linnaeus, 1758). Here, we present evidence of a white shark with a highly deformed pectoral fin that has been filmed twice over a five month period. Additionally, we discuss the possible functional consequences the white shark may have suffered and how this shark has most likely modified its behavior and survived during this time span.

On the morning of 27 August 2020, a juvenile white shark of unknown sex (C. Gauna pers. comm.) with a deformed left pectoral fin was observed via drone just off the coast of Santa Barbara, California, USA (Fig. 1a). The pectoral fin was intact but was bent up at nearly a 90° angle practically flush against the body. The shark appeared to be swimming in the upright position without any indication of it swimming on a rolled axis despite its pectoral fin deformity (Fig. 1a and Supporting Information Video S1). However, the shark appears to be putting forth increased effort just to swim in an irregular motion (non-thunniform) most likely due to its pectoral fin deformity (Supporting Information Video S1). In addition, it is unknown if this was a birth deformity or if the deformity was sustained later in life by some other cause (i.e., natural or human related). On the evening of 17 January 2021, almost five months after the first observation, the same individual was filmed in the same area again (Fig. 1b).

* Corresponding author: philsternes77@gmail.com

Downloaded from http://meridian.allenpress.com/scasbulletin/article-pdf/120/2/59/2930754/i2162-4534-120-2-59.pdf by guest on 12 December 2024

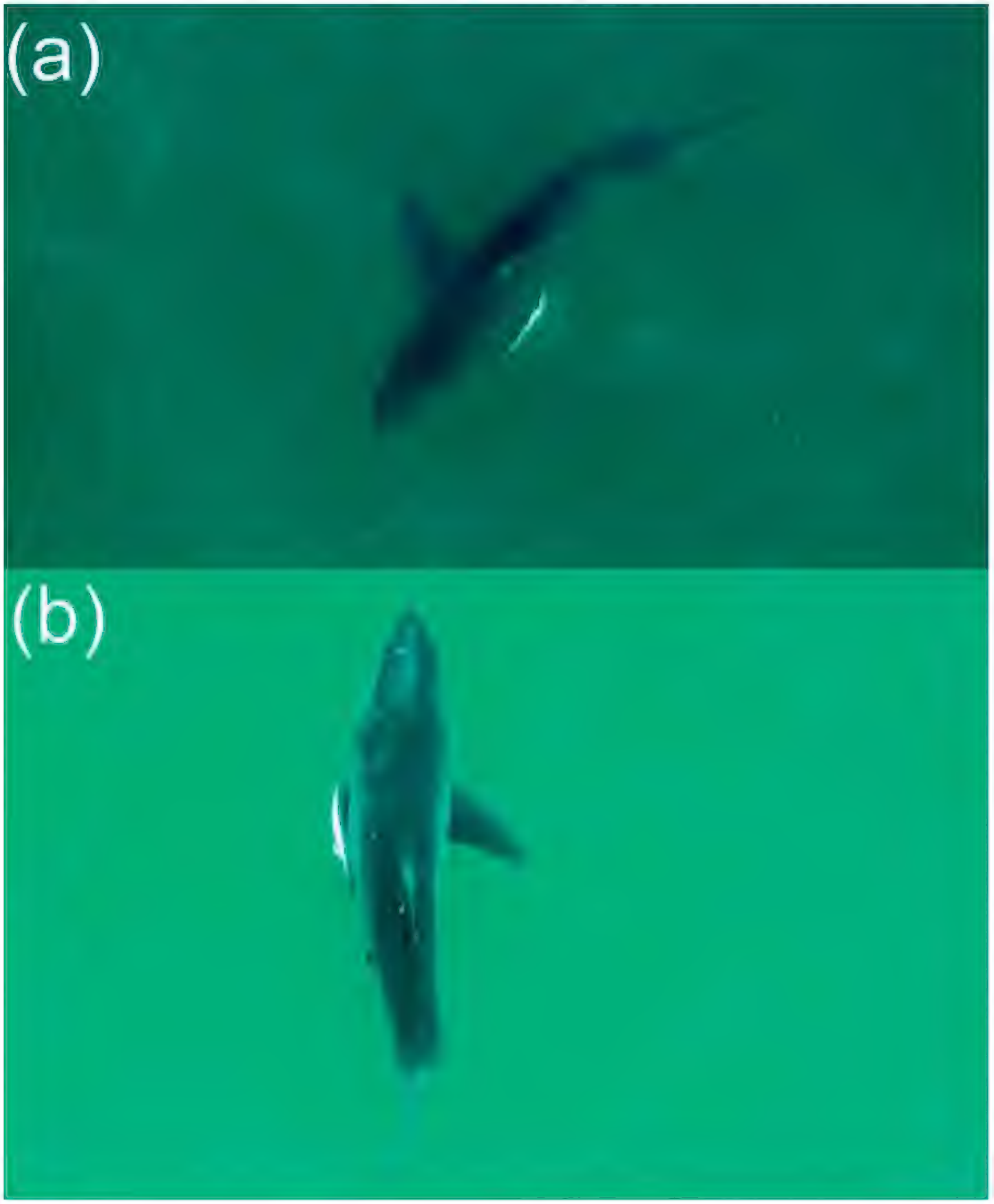

Fig. 1. A white shark (*C. carcharias*) with a deformed pectoral fin photographed off the coast of Santa Barbara, California in (a) August 2020 and (b) January 2021. Photo Credit: Carlos Gauna.

The pectoral fin deformity of the shark raises some interesting questions regarding the functional purpose of pectoral fins in highly pelagic fishes, such as white sharks. First, any swimming fish must maintain its pitch, roll, and yaw (Sfakiotakis et al. 1999) and the fins of fishes are crucial in maintaining these during their routine steady swimming (Lauder and Drucker 2004). A lack of a pectoral fin may lead to unsteady swimming or the fish swimming on its side or a rolled axis (Blake 2004; Maia et al. 2012). Next, it was previously thought pectoral fins were critical in generating lift (Harris 1936). However, for leopard,

Downloaded from http://meridian.allenpress.com/scasbulletin/article-pdf/120/2/59/2930754/i2162-4534-120-2-59.pdf by guest on 12 December 2024

Triakis semifasciata Girard, 1855, and bamboo, *Chiloscyllyium plagosium* (Anonymous [Bennett], 1830), sharks, the pectoral fins did not generate any lift forces, instead the fins can be oriented in different ways to move up and down in the water column (Wilga and Lauder 2000; 2001). It was shown the anterior body of both shark species were responsible for generating lift (Wilga and Lauder 2000; 2001). However, unlike bamboo and leopard sharks, white sharks have high aspect, stiffer pectoral fins. Thus, Lingham-Soliar (2005) suggested white shark pectoral fins must provide additional hydrodynamic lift as white sharks are pelagic highly migratory species with a much different body shape compared to that of benthic leopard and bamboo sharks. Lastly, sharks use their pectoral fins for turning and maneuvering especially for fine scale movement in the water (Hoffmann and Porter 2019).

Based on these functional aspects of shark pectoral fins, this raises some questions on the deformed white shark. The white shark appears to be swimming in the normal upright position and not on a rolled axis but it does appear to be swimming in an irregular motion and not routine steady swimming (Fig. 1 and Supporting Information Video S1). On the one hand, the loss of one pectoral fin has not disrupted the overall roll of the shark. However, the shark's routine steady swimming, or thunniform swimming, has been affected, implicating the pectoral fin is critical in that aspect. In addition, this suggests turning maneuvers have been greatly affected as well. Because it is drone footage, measuring the overall lift of the shark is not possible but the shark appears to be holding position in the water column. Additionally, both instances show the white shark at the surface and it is thus difficult to know how the shark is moving vertically in the water column.

White sharks are highly mobile predators that exhibit great bursts of speed (Klimley 1994; Watanabe et al. 2019). However, the deformed pectoral fin has clearly disrupted normal swimming behavior and most likely any burst speed behavior raising concerns on how this individual captures its prey or obtains food. This individual is a juvenile white shark (C. Gauna pers. comm.) and juveniles tend to favor pelagic and benthic teleosts as well as batoids (Grainger et al. 2020). Interestingly, the white sharks in this area are observed to be frequently feeding on bat rays (*Myliobatis californica* Gill, 1865) (C. Gauna pers. comm.). Future drone footage may confirm if this individual is indeed foraging on batoids in the area. Whereas batoids and pelagic teleosts are faster swimming prey, the injured white shark may be consuming much slower swimming benthic teleosts (Grainger et al. 2020). Another possibility is the white shark might be scavenging on whale carcasses a common behavior along California coast (Long and Jones 1996; Curtis et al. 2006).

Adult Eastern North Pacific white sharks are known to perform long distance migrations throughout their life (Jorgensen et al. 2010). These migrations might be important for either mating or foraging purposes (Weng et al. 2007). Nevertheless, the deformed white shark may be unable to perform any future migrations due to the increased effort put forth during its irregular swimming motion (Supporting Information Video S1). Future footage may reveal the home range of this shark and its migratory capabilities.

Any injured animal is subjected to higher predation risk as it likely has a decrease in performance for escape maneuvers (Lima and Dill 1990). Although adult white sharks in the Eastern North Pacific are top predators themselves, they have one natural predator, the killer whale (*Orcinus orca)* (Pyle et al. 1999). Because of this, Eastern North Pacific white sharks are known to vacate areas when killer whales are present, which are known to move up and down the California coast (Jorgensen et al. 2019). Thus, due to its possible decrease in locomotory capabilities and swimming efficiency, this injured white shark may be of high risk to future killer whale predation. On the other hand, Santa Barbara is an

Downloaded from http://meridian.allenpress.com/scasbulletin/article-pdf/120/2/59/2930754/i2162-4534-120-2-59.pdf by guest on 12 December 2024

aggregation site of juvenile white sharks as it provides possible protection against larger predators (Klimley 1985). Future documentation may reveal behavioral strategies of this unique individual and whether it leaves the protection of Santa Barbara.

A deformed juvenile white shark has been observed off the coast of Santa Barbara, CA, USA twice in a five month span. The peculiar deformity has not affected the overall posture of the shark, but it has affected the swimming motion of the shark. Thus, this indicates the loss of a pectoral fin does play a critical role in certain aspects of the white shark's swimming motion. This raises questions on how the individual has survived during the time span. The white shark may be capturing slower moving prey or scavenging. In addition, this white shark may not be able to perform long distance migrations as other white sharks in the region (Jorgensen et al. 2010). Lastly, this white shark may be of high risk of killer whale predation due to its decreased locomotor capabilities. Future footage and documentation may show future behavioral modifications, home range, and survivorship of this uniquely deformed white shark.

Acknowledgements

We deeply thank Carlos Gauna (TheMalibuArtist) for providing the photos and additional information on the injured white shark. We thank Kenshu Shimada for his additional insights and comments on white shark biology.

Literature Cited

Becerril-García, E.E., D. Bernot-Simon, M. Arellano-Martinez, F. Galván-Magaña, O. Santana-Morales, and E.M. Hoyos-Padilla. 2020. Evidence of interactions between white sharks and large squids in Guadalupe Island, Mexico. Sci. Rep., 10:17158.

Blake, R.W. 2004. Fish functional design and swimming performance. J. Fish Biol., 65:1193–1222.

Chin, A., J. Mourier, and J.L. Rummer. 2015. Blacktip reef sharks (*Carcharhinus melanopterus*) show high capacity of wound healing and recovery following injury. Conserv. Physiol., 3:cov062.

Curtis, T.H., J.T. Kelly, K.L. Menard, R.K. Laroche, R.E. Jones, and A.P. Klimley. 2006. Observations on the behavior of white sharks scavenging a whale carcass at Point Reyes, California. Calif. Fish Game., 92:113–124.

Grainger, R.G., V.M. Peddemors, D. Raubenheimer, and G.E. Machovsky-Capuska. 2020. Diet composition and nutritional breadth variability in juvenile white sharks (*Carcharodon carcharias*). Front. Mar. Sci., 7:1–20.

Harris, J.E. 1936. The role of the fins in the equilibrium of the swimming fish I. Wind-tunnel tests on a model of *Mustelus canis*. J. Exp. Biol., 13:476–493.

Hoffmann, S.L., and M.E. Porter. 2019. Body and pectoral fin kinematics during routine yaw turning in bonnethead sharks (*Sphyrna tiburo*). IOB., 1:1–15.

Jorgensen, S. et al. 2010. Philopatry and migration of Pacific white sharks. Proc. R. Soc. Lond. [Biol], 277:679–688.

———. et al. 2019. Killer whales redistribute white shark foraging pressure on seals. Sci. Rep., 9:6153.

Klimley, A.P. 1985. The areal distribution and autoecology of the white shark, *Carcharodon carcharias*, off the west coast of North America. Mem. Calif. Acad. Sci., 9:15–40.

———. 1994. The predatory behavior of the white shark. Am. Sci., 82:122–133.

Lauder, G.V., and E.G. Drucker. 2004. Morphology and experimental hydrodynamics of fish fin control surfaces. IEEE J. Ocean. Eng., 29:556–571.

Lima, S.L., and L.M. Dill. 1990. Behavioral decisions made under the risk of predation: a review and prospectus. Can. J. Zool., 68:619–640.

Lingham-Soliar, T. 2005. Caudal fin allometry in the white shark *Carcharodon carcharias*: implications for locomotory performance and ecology. Naturwissenschaften, 92:231–236.

Long, D.J., and R.E. Jones. 1996. White shark predation and scavenging on cetaceans in the Eastern North Pacific Ocean. Pp. 293–307 in Great White Sharks: The Biology of Carcharodon carcharias. (A.P. Klimley and P. G. Ainley, eds.) Academic Press.

Downloaded from http://meridian.allenpress.com/scasbulletin/article-pdf/120/2/59/2930754/i2162-4534-120-2-59.pdf by guest on 12 December 2024

Maia, A.M.R., C.A.D. Wilga, and G.V. Lauder. 2012. Biomechanics of locomotion in sharks, rays, and chimeras. Pp. 125–151 in Biology of Sharks and Their Relatives, second edition (J.C. Carrier, J.A. Musick, and M.R. Heithaus, eds.) CRC Press.

Maia, A., G.V. Lauder, and C.D. Wilga. 2017. Hydrodynamic function of dorsal fins in spiny dogfish and bamboo sharks during steady swimming. J. Exp. Biol., 220:3967–3975.

Mumby, P.J. 2019. Survival of a grey reef shark *Carcharhinus amblyrhynchos* without a dorsal fin. Fish Bio., 94:820–822.

Pratt, H.L. Jr., and J.C. Carrier. 2001. A review of elasmobranch reproductive behavior with a case study on the nurse shark, *Ginglymostoma cirratum*. Environ. Biol. Fish., 60:157–188.

Pyle, P., M.J. Schramm, C. Keiper, and S.D. Anderson. 1999. Predation on a white shark (*Carcharodon carcharias*) by a killer whale (*Orcinus orca*) and a possible case of competitive displacement. Mar. Mamm. Sci., 15:563–568.

Reif, W.E. 1978. Wound healing in sharks. Zoomorphologie, 90:101–111.

Roff, G., C. Doropoulos, A. Rogers, Y. Bozec, N.C. Krueck, E. Aurellado, M. Priest, C. Birrell and P.J. Mumby. 2016. The ecological role of sharks on coral reefs. TREE, 31:395–407.

Sfakiotakis, M., D.M. Lane, and B.C. Davies. 1999. Review of fishing swimming modes for aquatic locomotion. IEEE J. Ocean. Eng., 24:237–252.

Watanabe, Y.Y., N.L. Payne, J.M. Semmens, A. Fox, and C. Huveneers, 2019. Hunting behaviour of white sharks recorded by animal-borne accelerometers and cameras. MEPS, 621:221–227.

Weng, K.C., A.M. Boustany, P. Pyle, S.D. Anderson, A. Brown, and B.A. Block. 2007. Migration and habitat of white sharks (*Carcharodon carcharias*) in the eastern Pacific Ocean. Mar. Biol., 152: 877–894.

Wilga, C.D., and G.V. Lauder. 2000. Three-dimensional kinematics and wake structure of the pectoral fins during locomotion in leopard sharks *Triakis semifasciata*. J. Exp. Biol., 203:2261–2278.

Wilga, C. D., and G.V. Lauder. 2001. Functional morphology of the pectoral fin in bamboo sharks, *Chiloscyllium plagiosum*: benthic vs. pelagic station-holding. J. Morph., 249:195–209.

Womersley, F., J. Hancock, C.T. Perry, and D. Rowat. 2021. Wound-healing capabilities of whale sharks (*Rhincodon typus*) and implications for conservations management. Conserv. Physiol., 9(1):coaa120.

Downloaded from http://meridian.allenpress.com/scasbulletin/article-pdf/120/2/59/2930754/i2162-4534-120-2-59.pdf by guest on 12 December 2024

Bull. Southern California Acad. Sci.
120(2), 2021, pp. 64–87
© Southern California Academy of Sciences, 2021

A Redescription of *Lepeophtheirus longipes* Wilson, 1905 (Copepoda; Caligidae) Parasitic on Giant Sea Bass, *Stereolepis gigas* Ayres, 1859 (Polyprionidae), off California

Julianne Kalman Passarelli,[1]* Danny Tang,[2] and Larry G. Allen[3]

[1]*Cabrillo Marine Aquarium, 3720 Stephen M. White Drive, San Pedro, CA 90731, USA*
[2]*Environmental Laboratory and Ocean Monitoring Division, Orange County Sanitation District, 10844 Ellis Ave, Fountain Valley, CA 92708, USA*
[3]*California State University, Northridge, Department of Biology, 18111 Nordhoff St., Northridge, CA 91330, USA*

Abstract.—The giant sea bass (GSB), *Stereolepis gigas* Ayres, 1859, is the largest teleost (exceeding 2 m in length and 200 kg in weight) and megacarnivore found in California kelp forest communities. Overfishing of GSB in the late 1920s crashed the population off California and in 1996 it was classified as an International Union for Conservation of Nature (IUCN) critically endangered species. Recently, three GSB were collected off San Onofre, California and held at the Southern California Marine Institute in San Pedro. Two of the three GSB were infected with *Lepeophtheirus longipes* Wilson, 1905 (Siphonostomatoida; Caligidae), a poorly described species of parasitic copepod previously recorded from the GSB and purportedly on other fish hosts. In this study, a detailed redescription of the female and the first description of the male of *L. longipes* are provided and all records of *Lepeophtheirus longipes* are reviewed. The latter revealed that *L. longipes* is host specific to GSB. *Lepeophtheirus longipes* is distinguished from its congeners by a combination of female characters that includes: (1) genital complex with prominent posterolateral lobes and is about half the length of the cephalothorax and just over two times longer than the cylindrical, indistinctly 2-segmented abdomen; (2) an antennule with a small conical process on the proximal segment; (3) maxillule with an outer conical process at the base of the dentiform process; (4) sternal furca with pointed and slightly splayed tines; (5) first exopodal segment of leg 3 with a terminal spine; and (6) third exopodal segment of leg 4 with three unequal apical spines.

The giant sea bass (GSB), *Stereolepis gigas* Ayres, 1859 (Polyprionidae Bleeker, 1874), is the largest teleost and megacarnivore found in California, U.S.A. kelp bed communities. It ranges from Humboldt Bay, northern California to Oaxaca, southern Mexico, including the Gulf of California (Love and Passarelli 2020), but is most common from southern California southward along Baja California and into the Gulf of California (Allen and Andrews 2012). It forms spawning aggregations during the summer months (July-September) (Shane et al. 1996) and is often found in kelp forests on rocky reefs as adults, while juveniles are found at sandy bottom areas (Domeier 2001).

These large, demersal teleosts reach lengths longer than 2 m, weights greater than 200 kg, ages of up to 76 yrs, and are apex predators (Horn and Ferry-Graham 2006; Allen

* Corresponding author: julianne.passarelli@lacity.org

Downloaded from http://meridian.allenpress.com/scasbulletin/article-pdf/120/2/64/2930772/i2162-4534-120-2-64.pdf by guest on 12 December 2024

and Andrews 2012; Hawk and Allen 2014; Chabot et al. 2015; House et al. 2016; Allen 2017). Like many apex predators, these fish grow slowly and were historically easily overfished. At the end of the 1920s, the commercial fishing fleet out of San Pedro, California was growing and began fishing (gill netting and hand lining) GSB in earnest, often targeting their spawning aggregations in the summer months. This practice led to the near complete demise of the GSB fishery off California by 1934 (Croker 1937). Since 1934, the only appreciable commercial landings of GSB were from off Baja California. Their commercial landings and populations decreased to almost nothing until, in 1982, the Mexican government prohibited the commercial take of this species from Mexican waters. In the same year, the California Department of Fish and Game (now the California Department of Fish and Wildlife - CDFW) placed a complete moratorium on the recreational catch, and the commercial catch was limited to two fish and later to one per trip. In fact, the population of GSB dwindled so rapidly during the 20th century that they are now on the International Union for Conservation of Nature (IUCN) Red List as a critically endangered species (Musick et al. 2000; Cornish 2004). Then, in 1990, the voters of California passed Proposition 132, which banned all gill netting from inshore waters and up to three miles offshore. Its implementation in 1994 has benefited some predatory fishes, including GSB (Pondella and Allen 2008), and the GSB population now appears to be in the early stages of recovery (Allen 2017).

Recently, three GSB were captured off southern California and then transported to the Southern California Marine Institute (SCMI) in San Pedro for morphological studies. Two of the three GSB were infected with at least 60 individuals of *Lepeophtheirus longipes* Wilson, 1905 (Siphonostomatoida Burmeister, 1835; Caligidae Burmeister, 1835), a species of parasitic copepod that was poorly described based on two females (host and locality unknown) and later recorded from GSB, kelp bass, *Paralabrax clathratus* (Girard, 1854) (Serranidae Swainson, 1839), and treefish, *Sebastes serriceps* (Jordan & Gilbert, 1880) (Scorpaenidae Risso, 1826), captured off the California coast and from other fish hosts caught in far-flung localities (Table 1). *Lepeophtheirus* von Nordmann, 1832 is the second most speciose genus of the family Caligidae, with 125 valid species and 2 recognized subspecies (Walter and Boxshall 2021). Although members of *Lepeophtheirus* (and other caligid genera) are predominantly external parasites of marine fishes (Dojiri and Ho 2013), the adult female of *Lepeophtheirus semicossyphi* Yamaguti, 1939 and *Lepeophtheirus alvaroi* Suárez-Morales and Gasca, 2012 are known to occur in the plankton (Venmathi Maran et al. 2016).

Due to the small population size and protection status of the GSB host, reports in the primary literature of *L. longipes* in California have been sparse (Wilson 1908, 1921a; Hobson 1971). We take this opportunity to provide a redescription by modern standards of *L. longipes* based on the new material and to review all records of *L. longipes*.

Materials and Methods

Three GSB, ranging from 1.15-1.39 m Total Length and 28.9-49.5 kg, were collected by hook and line (CDFW Scientific Collecting Permit #000032 issued to LGA) approximately 3 km offshore from an onshore point slightly southeast of the San Onofre Nuclear Generating Station (33°20.612'N, 117°34.132'W) in August and September 2017 (Table 2). All three fish were subsequently transported alive to the SCMI where they were held in captivity in tanks.

Downloaded from http://meridian.allenpress.com/scasbulletin/article-pdf/120/2/64/2930772/i2162-4534-120-2-64.pdf by guest on 12 December 2024

Table 1. Historical records of fish hosts and localities for *Lepeophtheirus longipes*.

Host family	Host species	Locality	Reference
Unknown	Unknown	Unknown	Wilson (1905)
Polyprionidae	*Stereolepis gigas* Ayres, 1859	La Jolla, California, U.S.A.	Wilson (1908)
Serranidae	*Paralabrax clathratus* (Girard, 1854)	Catalina Island, U.S.A.	Wilson (1921a)[a]
Sciaenidae	*Argyrosomus regius* (Asso, 1801) (as *Sciaena aquila*)	Mauritania; Mediterranean Sea from Gibraltar to Cape Bon, Tunisia	Brian (1924)[b]; Rose and Vaissière (1953)[c]
	Argyrosomus regius (Asso, 1801)	Mediterranean Sea	Raibaut et al. (1998)[d]
Echeneidae	*Echeneis naucrates* Linnaeus, 1758	Port Etienne, Mauritania	Brian (1924)[b]
Haemulidae	*Plectorhinchus mediterraneus* (Guichenot, 1850) (as *Diagramma mediterraneum*)	Mauritania	Brian (1924)[b]
Scorpaenidae	*Sebastes serriceps* (Jordan & Gilbert, 1880)	Southern California, U.S.A.	Hobson (1971)[e]
Scorpaenidae	*Sebastes maliger* (Jordan & Gilbert, 1880) (as *Sebastodes maliger*)	San Juan Islands, Washington, U.S.A.	Nichols (1975)[f]

[a] Copepod specimens were reported as *L. longipes*, but examination of voucher specimens revealed they are *Lepeophtheirus constrictus* Wilson, 1908.

[b] Copepod specimens were reported as *L. longipes*, but examination of digital photographs of these specimens revealed they are not conspecific with *L. longipes*.

[c] The locality for this record is provided in Rose and Vaissière (1952). Also, this record of *L. longipes* from *A. regius* is doubtful.

[d] This record of *L. longipes* from *A. regius* is doubtful.

[e] Copepod specimens were reported as *L. longipes*, but they were likely *Lepeophtheirus paulus* Cressey, 1969.

[f] Copepod specimens were reported as *L. longipes*, but examination of voucher specimens revealed they are *Lepeophtheirus oblitus* Kabata, 1973.

All three fish were treated with a freshwater dip and detached copepods were collected and then preserved in 70% ethanol. Two of the three fish were infected: fish designated SOK-1 had few copepods while SOK-2 harbored many copepods (LGA, personal observation). Microscopic examination, measurements, and illustrations of copepod

Table 2. Giant sea bass collection information.

Specimen	Date of Capture	Location	Vessel	Time of Day	Total Length (m)	Weight (kg)	Disposition
SOK-1	8/29/17	San Onofre Kelp	MV Reel Fun	10:45 AM	1.39	49.5	Tank at SCMI expired 9/11/17
SOK-2	8/29/17	San Onofre Kelp	MV Reel Fun	11:15 AM	1.15	28.9	Tank at SCMI
SOK-3	9/28/17	San Onofre Kelp	SCE Parker 2520	11:30 AM	1.24	36.1	Tank at SCMI

Downloaded from http://meridian.allenpress.com/scasbulletin/article-pdf/120/2/64/2930772/i2162-4534-120-2-64.pdf by guest on 12 December 2024

specimens follow Passarelli and Tang (2017). In the description, length measurements are provided first, followed by width measurements; all measurements given are expressed as the mean followed by the range in parentheses. Morphological terminology follows Huys and Boxshall (1991) and Dojiri and Ho (2013). Fish classifications and names conform to Froese and Pauly (2020) and Love and Passarelli (2020). Voucher specimens are deposited at the Crustacea Department of the Natural History Museum of Los Angeles County (LACM), Los Angeles, California, and at Cabrillo Marine Aquarium (CMA), San Pedro, California.

The following specimens of *L. longipes* deposited in the National Museum of Natural History (USNM), Smithsonian Institution, Washington, D.C., U.S.A., and the Muséum national d'Histoire naturelle (MNHN), Paris, France, were examined for comparative purposes:

1. Preserved material comprising 1 female syntype (USNM 12488), host, locality, and collection date unknown.
2. Preserved material comprising 27 females (USNM 38567), ex *Stereolepis gigas*, La Jolla, California, U.S.A., May 18, 1906, collected by J. F. McClendon, identified by C. B. Wilson.
3. Preserved material comprising 5 females (USNM 74301), ex outside of jewfish (=giant sea bass), La Jolla, California, U.S.A., July 1907, collected by J. F. McClendon, identified by C. B. Wilson.
4. Preserved material comprising 6 females and 3 males (USNM 49779), ex mouth of *Paralabrax clathratus*, Crescent Bay, Santa Catalina Island, U.S.A., June 19, 1913, collected by P. S. Barnhart, identified by C. B. Wilson.
5. Preserved material comprising 7 females and 1 male (USNM 180909), ex surface of *Sebastes maliger* (as *Sebastodes maliger*), San Juan Islands, Friday Harbor, Washington, U.S.A., collection date unknown, identified by R. F. Cressey.
6. Five digital photographs of 1 female (MNHN-IU-2007-2964 (=MNHN-Cp53)), ex mouth of *Echeneis naucrates*, Mauritania, 1923, collected by T. Monod, identified by A. Brian.
7. Five digital photographs of 1 female (MNHN-IU-2007-2975 (=MNHN-Cp54)), ex *Plectorhinchus mediterraneus* (as *Diagramma mediterraneum*), Mauritania, May 1923, collected by T. Monod, identified by A. Brian.
8. Three digital photographs of 1 male (MNHN-IU-2007-2986 (=MNHN-Cp55)), ex tail of *Argyrosomus regius* (as *Sciaena aquila*), Mauritania, May 1923, collected by T. Monod, identified by A. Brian.
9. Six digital photographs of 2 females (MNHN-IU-2007-3008 (=MNHN-Cp57)), ex gills of *Argyrosomus regius* (as *Sciaena aquila*), Mauritania, April 1923, collected by T. Monod, identified by A. Brian.

Digital photographs of the maxillulary dentiform process and the distal exopodal segment of leg 1 (both appendages mounted on the same slide) of the holotype female of *Lepeophtheirus interitus* Wilson, 1921, deposited in the Swedish Museum of Natural History (SMNH-98034), were also examined for comparative purposes.

Results

Lepeophtheirus longipes Wilson, 1905
(Figs. 1-6)

Downloaded from http://meridian.allenpress.com/scasbulletin/article-pdf/120/2/64/2930772/i2162-4534-120-2-64.pdf by guest on 12 December 2024

Material examined. 36 ovigerous females (3 dissected), 4 mature non-ovigerous females, 16 immature females, and 4 males (1 dissected), ex 1 *Stereolepis gigas*, off San Onofre, California, U.S.A., August 29, 2017, collected by L. G. Allen. Six females and 1 male (LACM:DISCO:19981) deposited at LACM; 6 females and 1 male (CMA 2020.04.0003) deposited at CMA.

Description of adult female. Body (Fig. 1A) 8.27 (8.10-8.53) mm long (excluding caudal setae) (n = 4). Cephalothoracic shield subcircular, slightly longer than wide [4.36 (4.30-4.43) mm × 4.03 (3.98-4.10) mm], with well-developed paired frontal plates; posterior margin of thoracic zone extending beyond posterior limit of lateral zone; hyaline membrane present along margin of frontal plates and lateral zones. Free fourth pedigerous somite about two times wider than long [0.72 (0.70-0.73) mm × 1.54 (1.50-1.60) mm] and indistinctly separated from genital complex. Genital complex slightly longer than wide [2.24 (2.18-2.40) mm × 1.92 (1.79-2.08) mm], about half the length of cephalothoracic shield and slightly over two times longer than abdomen, with prominent posterolateral processes and numerous spiniform sensilla (Fig. 4C). Abdomen indistinctly separated from genital complex, composed of 2 indistinct somites, 631 (610-650) μm × 480 (460-500) μm and 368 (340-400) × 455 (430-475) μm, respectively. Caudal ramus (Fig. 1B) longer than wide [310 (280-330) μm × 183 (170-195) μm], with 1 unipinnate and 5 plumose setae (seta I absent) plus short row of setules along inner distal margin; seta II situated on ventral surface near insertion of seta III. Egg sacs (not figured) uniseriate.

Antennule (Fig. 1C) 2-segmented. Proximal segment longer than distal segment, bearing 1 small bifid process on posterodistal corner and 1 small conical process plus 27 setae (25 hirsute and 2 variably ornamented—see Variability section below) along anterior margin. Distal segment cylindrical, bearing 12 naked setae and 2 aesthetascs (2 setae near posterodistal corner share a common base; 1 apical seta and 1 apical aesthetasc share a common base).

Antenna (Fig. 1D) 3-segmented, comprising coxa, basis and 1-segmented endopod incorporating distal claw; situated on pedestal. Coxa with acuminate, posteriorly-directed process. Basis stout, with corrugated surface on inner distal corner and 1 corrugated adhesion pad (Fig. 1E) on dorsolateral surface. Endopod long, uncinate, bearing 1 finely spinulate proximal seta and 1 naked seta at middle of claw.

Postantennal process (Fig. 1F) recurved, with pair of setulose papillae on base and 1 setulose papilla posterior to base.

Mandible (Fig. 2A) modified into elongate stylet bearing distolateral hyaline membrane and 12 distomedial teeth.

Maxillule (Fig. 2B) composed of trisetose papilla and bifid dentiform process; latter with small, proximolateral conical process and subequal tines (outer tine slightly more curved than inner tine).

Maxilla (Fig. 2C), brachiform, 2-segmented, composed of elongate, unarmed syncoxa and slender basis. Basis with flabellum at mid-length plus long apical calamus and shorter subapical canna; calamus with finely serrated membranes along anterior margin; canna with finely serrated posterior margin.

Maxilliped (Fig. 2D-E) large, subchelate, 3-segmented, comprising long protopod (corpus) and subchela consisting of free endopodal segment (shaft) and claw. Protopod with small, semispherical process in myxal area plus 3 patches of crescentic denticles and 1 tiny element on anterior surface. Shaft with tiny distal element on posterior surface. Claw with naked proximal seta on posterior surface.

Downloaded from http://meridian.allenpress.com/scasbulletin/article-pdf/120/2/64/2930772/i2162-4534-120-2-64.pdf by guest on 12 December 2024

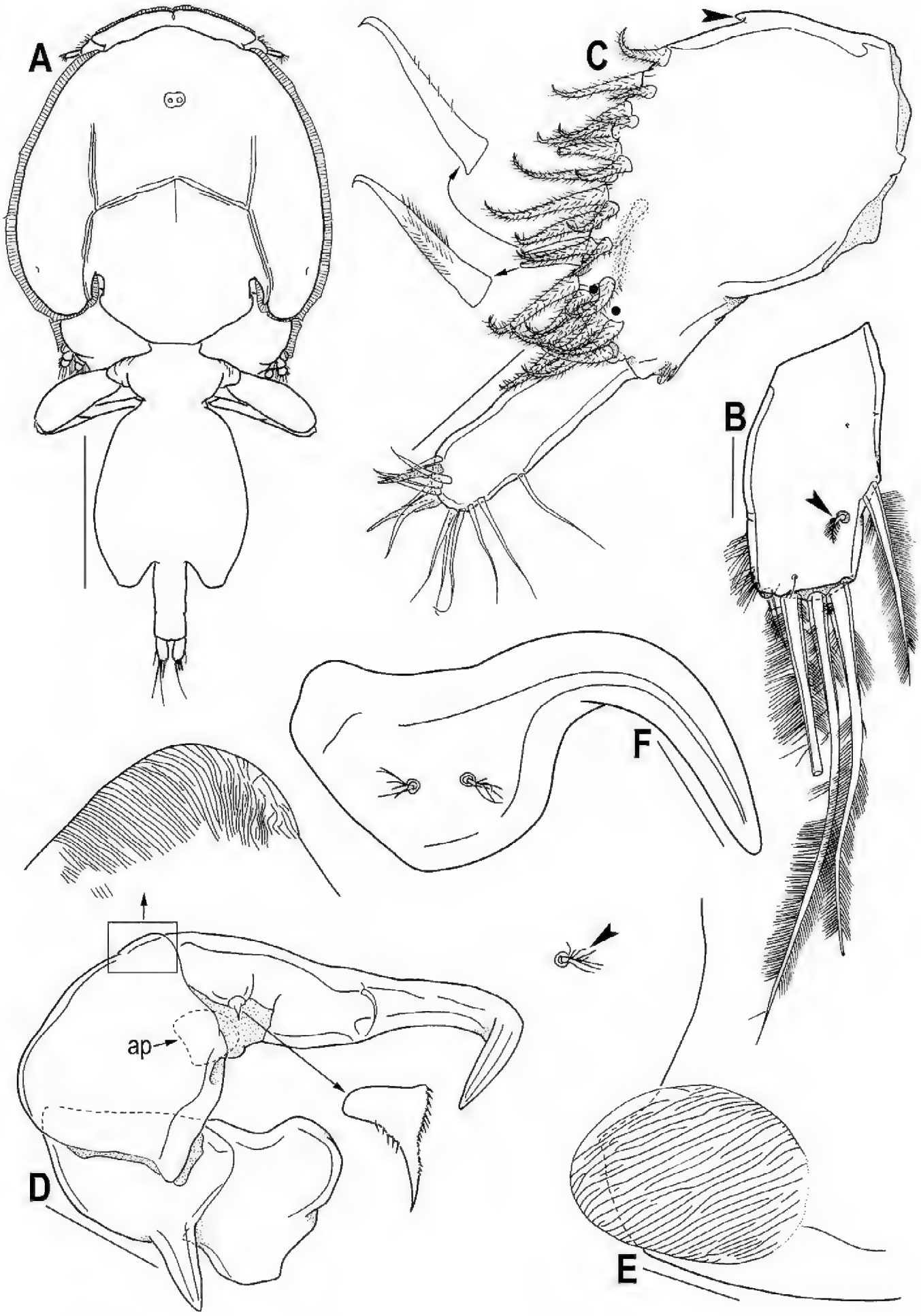

Fig. 1. *Lepeophtheirus longipes* Wilson, 1905, adult female. A) Habitus, dorsal; B) Left caudal ramus (arrowhead indicates seta II), ventral; C) Right antennule with detail of two subapical setae inserted on dorsal surface of anterior margin, black circles indicating position of additional setae on male antennule, and arrowhead indicating conical process on proximal segment, ventral; D) Left antenna with detail of anterodistal corner of second segment (ap = adhesion pad) and proximal seta on third segment, ventral; E) Adhesion pad on posterodistal corner of second segment of left antenna, dorsal; F) Postantennal process (arrowhead indicates multifurcate sensillum on ventral surface of cephalothorax), ventral. Scale bars: 2.00 mm for A; 100 μm for B, F; 150 μm for C; 200 μm for D; 50 μm for E.

Downloaded from http://meridian.allenpress.com/scasbulletin/article-pdf/120/2/64/2930772/i2162-4534-120-2-64.pdf by guest on 12 December 2024

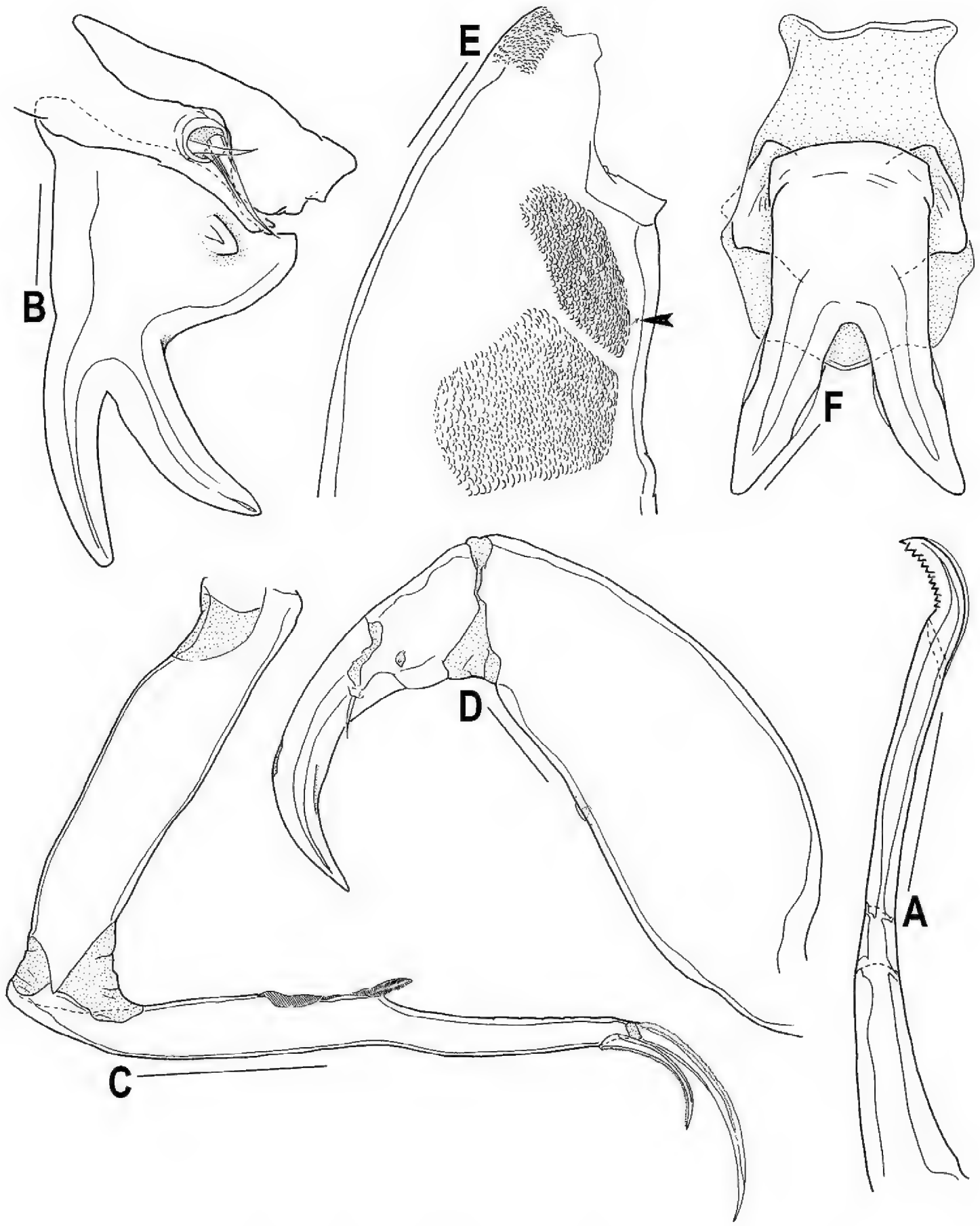

Fig. 2. *Lepeophtheirus longipes* Wilson, 1905, adult female. A) Right mandible, anterior; B) Left maxillule, ventral; C) Left maxilla, posterior; D) Left maxilliped, posterior; E) Distal half of protopod of left maxilliped (arrowhead indicates minute inner element), anterior; F) Sternal furca, anterior. Scale bars: 100 μm for A, B, E, F; 300 μm for C; 150 μm for D.

Tines of sternal furca (Fig. 2F) as long as box, splayed apart, furnished with short hyaline flange on outer and inner margins, and pointed at tip.

Legs 1 to 3 (Figs. 3A, E, G) biramous; leg 4 (Fig. 4A) uniramous. Armature formula of legs 1-4 is shown in Table 3.

Downloaded from http://meridian.allenpress.com/scasbulletin/article-pdf/120/2/64/2930772/i2162-4534-120-2-64.pdf by guest on 12 December 2024

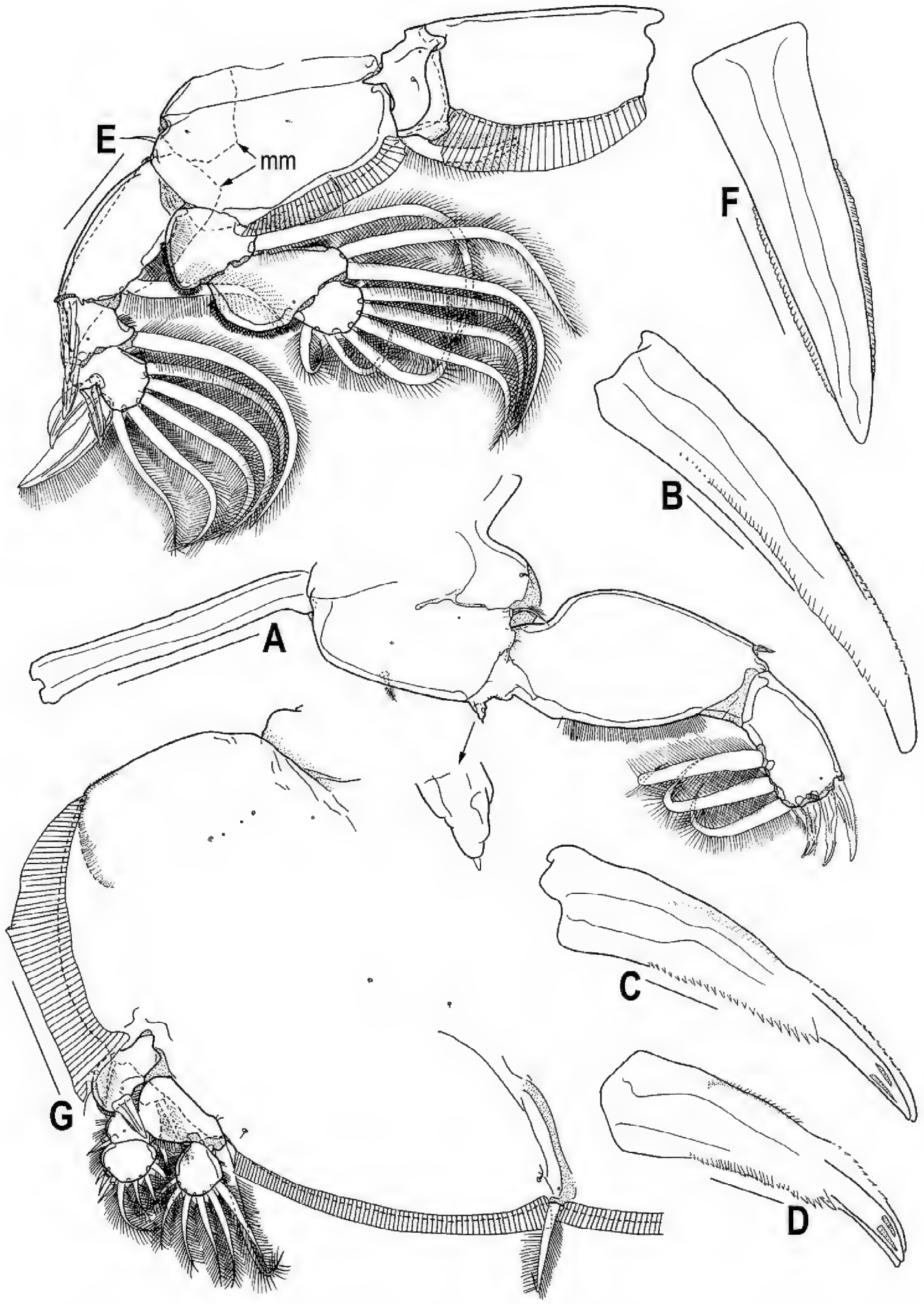

Fig. 3. *Lepeophtheirus longipes* Wilson, 1905, adult female. A) Left leg 1 with detail of endopod, anterior; B) Outer apical spine on second exopodal segment of left leg 1, anterior; C) Middle apical spine on second exopodal segment of left leg 1, anterior; D) Inner apical spine on second exopodal segment of left leg 1, anterior; E) Right leg 2 (mm = marginal membrane), anterior; F) Outer spine on middle exopodal segment of right leg 2, anterior; G) Right leg 3, ventral. Scale bars: 300 μm for A, G; 25 μm for B, C, D; 250 μm for E; 50 μm for F.

Downloaded from http://meridian.allenpress.com/scasbulletin/article-pdf/120/2/64/2930772/i2162-4534-120-2-64.pdf by guest on 12 December 2024

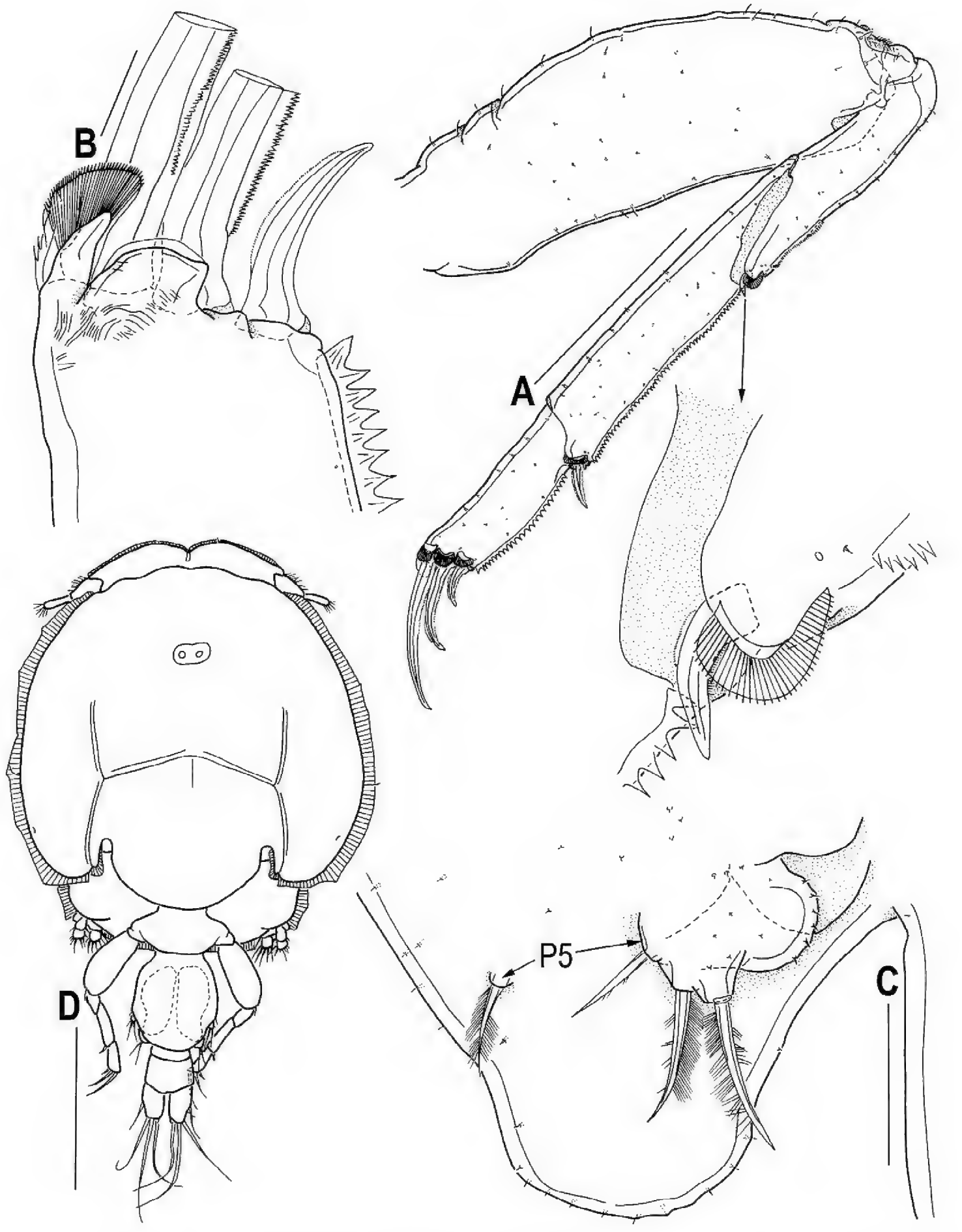

Fig. 4. *Lepeophtheirus longipes* Wilson, 1905, adult female (A-C) and adult male (D). A) Left leg 4 with detail of outer spine on first exopodal segment, ventral; B) Tip of third exopodal segment of left leg 4, dorsal; C) Posterolateral process of genital complex showing leg 5 (P5), ventral; D) Habitus, dorsal. Scale bars: 600 μm for A; 50 μm for B; 200 μm for C; 1.00 mm for D.

Downloaded from http://meridian.allenpress.com/scasbulletin/article-pdf/120/2/64/2930772/i2162-4534-120-2-64.pdf by guest on 12 December 2024

Table 3. Armature on legs 1-4 (Roman numerals = spines; Arabic numerals = setae).

	Coxa	Basis	Exopod	Endopod
Leg 1*	0-0	1-1	I-0; 0,III+1,3	vestigial
Leg 2	0-1	1-0	I-1; I-1; II,I,5	0-1; 0-2; 6
Leg 3*	0-1	1-0	I-1; I-1; II,I,4	0-1; 6
Leg 4*	0-0	1-0	I-0; I-0; 0,III,0	absent

*Although the coxa and basis are fused to form a protopod in this leg, these segments are treated separately in this Table.

Leg 1 (Fig. 3A) intercoxal sclerite naked and elongate. Protopod with 1 outer and 1 inner plumose setae, 1 proximolateral setulose papilla, and 2 surface pores. First exopodal segment with 1 small, naked outer spine and inner row of setules. Second exopodal segment with 3 apical spines (inner spine shortest), 1 apical seta, 3 inner plumose setae, surface pore near apical margin, and pectinate membrane at base of each apical spine; outer apical spine (Fig. 3B) with row of tiny denticles along distal half of anterior margin and row of small denticles along posterior margin; middle and inner apical spines (Fig. 3C-D) each with an accessory process and 2 rows of tiny denticles along anterior margin and row of larger denticles along posterior margin; apical seta plumose and as long as inner apical spine. Endopod vestigial, bearing 1 tiny apical element.

Leg 2 (Fig. 3E) intercoxal sclerite subquadrate, with hyaline membrane along distal margin. Coxa with 1 inner plumose seta plus 1 surface pore and 1 short sensillum on anterior surface. Basis with 1 outer naked seta, 2 surface pores, 1 large inner sensillum, large hyaline membrane along inner margin, and membrane on posterolateral surface. Exopod 3-segmented, with large hyaline membrane covering posterior surface of ramus. First segment with outer distal spine furnished with pectinate membrane at base, 1 inner plumose seta, and inner row of setules. Second segment with 1 outer distal spine, 1 surface pore, 1 inner plumose seta, and inner row of setules. Third segment with 3 outer spines, 5 inner plumose setae, and inner row of setules; middle outer spine with hyaline membrane along outer margin; outer distal spine with hyaline membrane along outer margin and row of setules along inner margin. Spine on first two exopodal segments and proximal outer spine on third exopodal segment each with finely serrated margins (Fig. 3F). Endopod 3-segmented. First segment with several rows of setules on outer margin and 1 inner plumose seta. Second segment with multiple rows of setules along outer margin, 1 surface pore, 2 inner plumose setae, and short row of setules along inner margin. Third segment with proximolateral row of setules, 6 plumose setae, and proximomedial row of setules.

Leg 3 (Fig. 3G) protopod large, modified to form apron, with 1 outer plumose seta situated near insertion of exopod, 1 inner plumose seta near large intercoxal sclerite, 1 proximolateral corrugated pad on dorsal surface, 3 marginal membranes, tiny sensilla scattered on ventral surface, and 2 widely separated sensilla along posterior margin. Exopod 3-segmented, ramus not extending beyond distal margin of second endopodal segment. First segment with 1 inner plumose seta, 1 apical spine reflexed over second segment and ornamented with sclerotized flange along outer margin, and 1 surface pore, several sensilla and sclerotized flange on outer basal swelling. Second segment with 1 outer naked spine, 1 inner plumose seta, 1 surface pore, and setules along outer and inner margins. Third segment with 3 naked spines, 4 plumose setae, and setules along outer and

Downloaded from http://meridian.allenpress.com/scasbulletin/article-pdf/120/2/64/2930772/i2162-4534-120-2-64.pdf by guest on 12 December 2024

inner margins. Endopod 2-segmented. First segment with 1 inner plumose seta and outer row of setules. Second segment with 6 plumose setae and setules along outer and inner margins.

Leg 4 (Fig. 4A) protopod with 1 distolateral plumose seta and numerous sensilla (combination of long and thin plus tiny and spiniform) scattered on the surface. Exopod 3-segmented, longer than protopod, with each segment ornamented with many tiny, spiniform sensilla. First exopodal segment with short row of serrations along outer distal third of segment and crescentic pectinate membrane at base of small, outer spine furnished with fine spinules along both margins. Second exopodal segment longer than other two segments (based on length of inner margin), with serrations along outer margin and crescentic pectinate membrane at base of outer distal spine furnished with fine spinules along both margins. Third exopodal segment with 3 unequal apical spines; outer spine about one-half length of middle spine, furnished with fine spinules along both margins and crescentic pectinate membrane at its base; middle spine about two-thirds length of inner spine, with fine spinules along both margins, crescentic pectinate membrane on ventral side of its base, and rhomboid process equipped with an apical hyaline flange on dorsal side of its base (Fig. 4B); inner spine with fine spinules along outer margin, crescentic pectinate membrane on ventral side of its base, and digitiform process furnished with apical pectinate membrane on dorsal side of its base (Fig. 4B).

Leg 5 (Fig. 4C) vestigial, situated proximally on ventral surface of posterolateral lobe of genital complex, and comprised of small setiferous papilla near outer margin and broad trisetose lobe near juncture of abdomen; broad lobe with spiniform sensilla and finely serrated flange at base of inner apical seta.

Leg 6 (not figured) rudimentary, represented by unarmed genital operculum at gonopore opening.

Description of adult male. Body (Fig. 4D) 3.49 (3.43-3.55) mm long (excluding caudal setae) (n = 4). Cephalothoracic shield orbicular, slightly longer than wide [2.23 (2.20-2.28) mm × 2.06 (1.96-2.13) mm], ornamented as in female. Free fourth pedigerous somite about twice as wide as long [265 (240-285) μm × 605 (580-630) μm]. Genital complex slightly longer than wide [575 (530-610) μm × 533 (520-545) μm]. Abdomen composed of 2 somites, 75 (60-80) μm × 243 (220-260) μm] and 190 (180-200) μm × 294 (270-305) μm], respectively. Caudal ramus (Fig. 5A) longer than wide [219 (210-225) μm × 138 (130-140) μm], with 6 plumose setae and inner row of setules; seta II situated on outer margin near insertion of seta III.

All appendages as in female, except for the following. Antennule with 2 additional setae on ventrodistal surface of proximal segment (position of each seta indicated by black circle in Fig. 1C). Antenna (Fig. 5B-C) 3-segmented, comprising coxa, basis, and 1-segmented endopod incorporating distal claw. Coxa with short row of fine striations plus large corrugated pad on posterior side and row of fine striations on anterior side. Basis with 4 corrugated pads on posterior side and 2 corrugated pads plus 1 long and 1 short rows of fine striations on anterior side. Endopod forming robust recurved claw bearing 2 proximal naked setae, 1 proximal accessory claw, sclerotized flange on each side of claw, and 1 small projection distal to sclerotized flange on anterior side. Maxillule (Fig. 5D) with rounded basal process, corrugated accessory process, and inner hyaline element on dentiform process. Postoral process (Fig. 5D) elongate and corrugated. Protopod of maxilliped (Fig. 5E) with conical process equipped with 1 spiniform element in myxal area and 1 medial surface pore. Tines of sternal furca (Fig. 5F) with rounded tip. Third exopodal segment of leg 4 (Fig. 6A) with smaller process and smaller pectinate membrane on dorsal side of base of

Downloaded from http://meridian.allenpress.com/scasbulletin/article-pdf/120/2/64/2930772/i2162-4534-120-2-64.pdf by guest on 12 December 2024

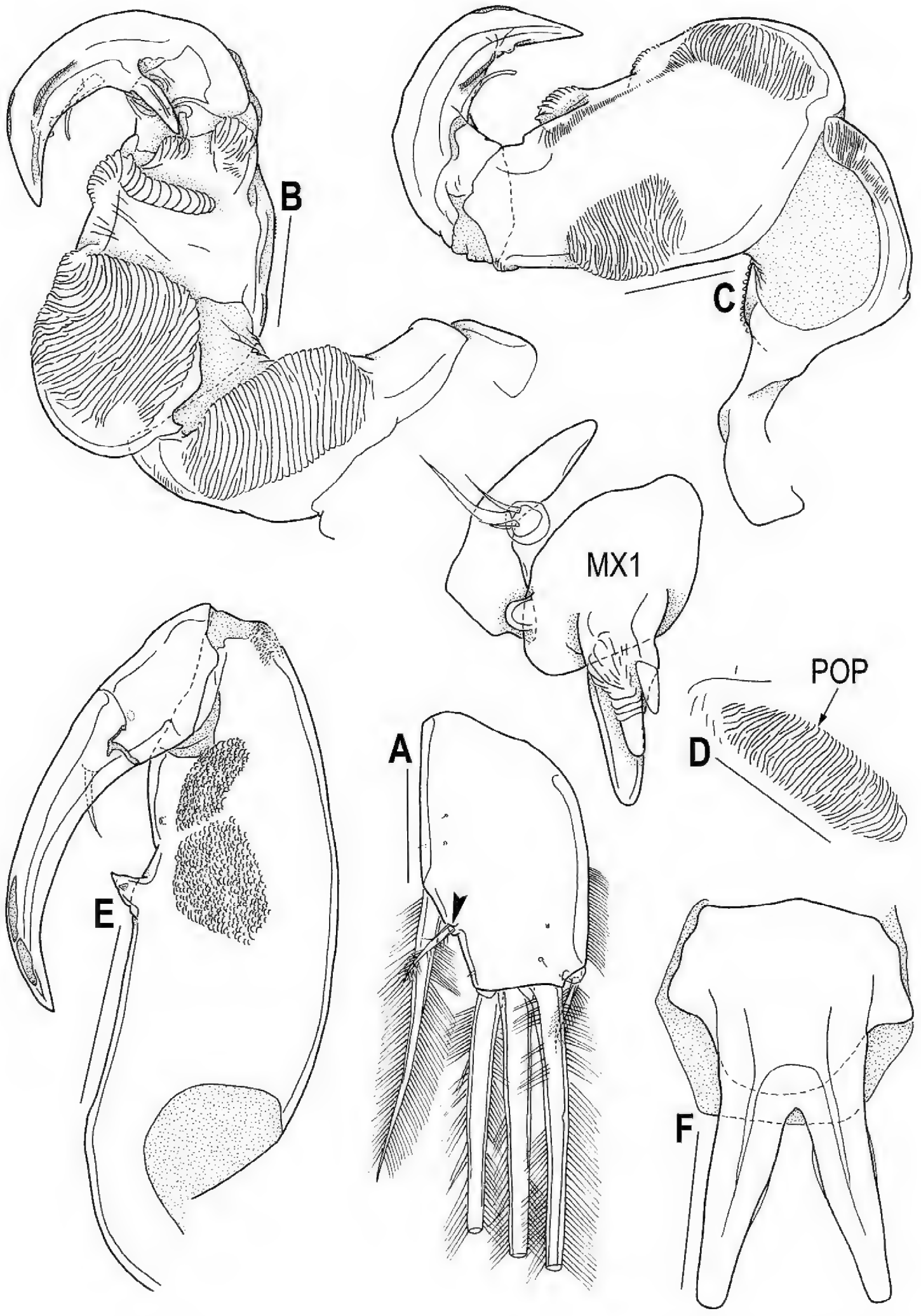

Fig. 5. *Lepeophtheirus longipes* Wilson, 1905, adult male. A) Right caudal ramus (arrowhead indicates seta II), ventral; B) Left antenna, posterior; C) Left antenna, anterior; D) Right maxillule (MX1) and postoral process (POP), ventral; E) Right maxilliped, anterior; F) Sternal furca, anterior. Scale bars: 100 μm for A, B, C, D, F; 150 μm for E.

Downloaded from http://meridian.allenpress.com/scasbulletin/article-pdf/120/2/64/2930772/i2162-4534-120-2-64.pdf by guest on 12 December 2024

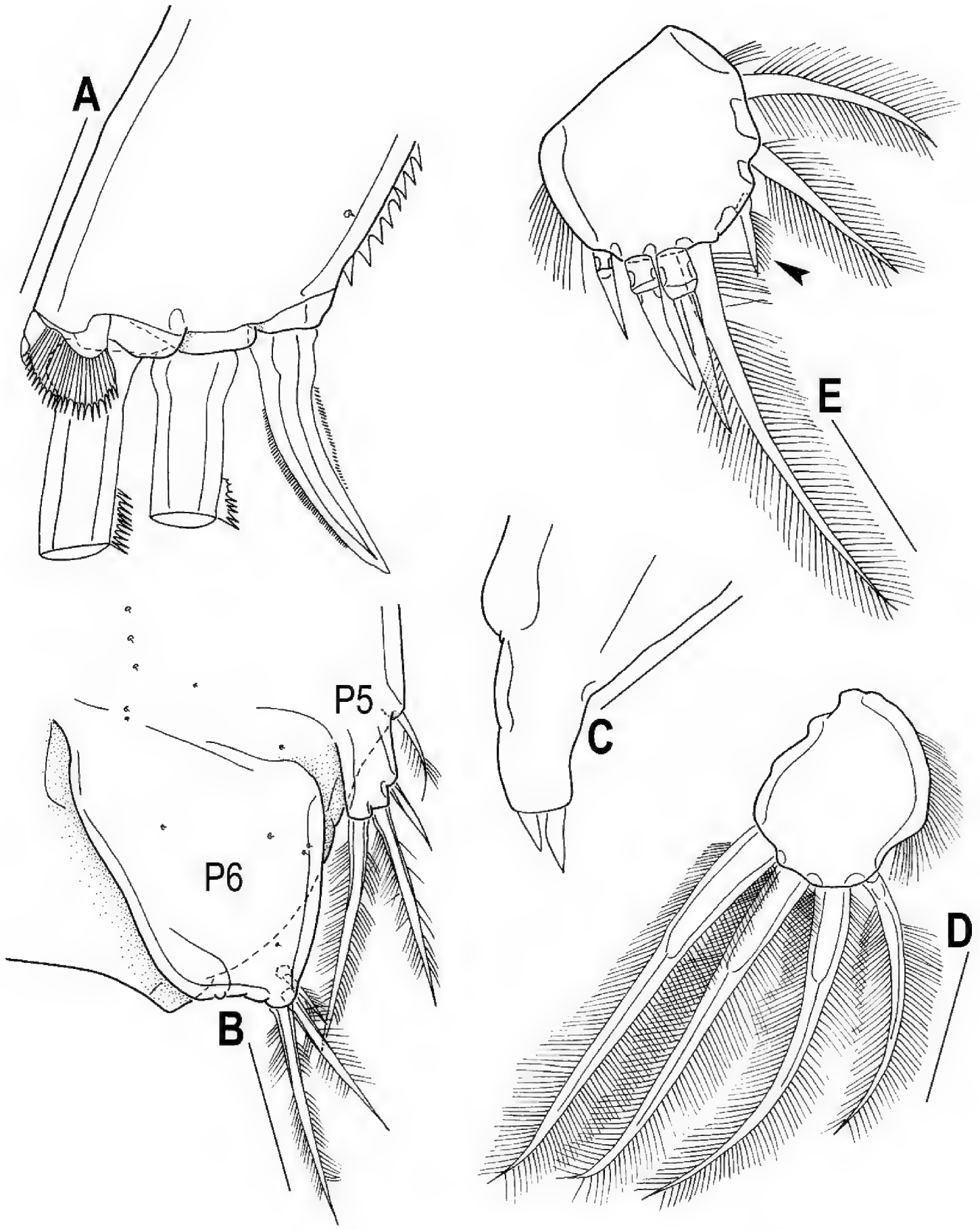

Fig. 6. *Lepeophtheirus longipes* Wilson, 1905, adult male (A, B, E) and adult female (C, D). A) Tip of third exopodal segment of right leg 4, dorsal; B) Left legs 5 (P5) and 6 (P6), ventral; C) Endopod on right leg 1, anterior; D) Second endopodal segment of left leg 3, ventral; E) Third exopodal segment of right leg 3 (arrowhead indicates abnormal seta), ventral. Scale bars: 50 μm for A; 100 μm for B, D; 25 μm for C; 50 μm for E.

middle and inner spines, respectively. Leg 5 (Fig. 6B) vestigial, comprising 1 plumose seta on surface of genital complex and 1 naked spiniform seta plus 2 plumose setae on rectangular segment. Leg 6 (Fig. 6B) forming genital operculum, armed with 3 plumose setae on outer distal corner.

Downloaded from http://meridian.allenpress.com/scasbulletin/article-pdf/120/2/64/2930772/i2162-4534-120-2-64.pdf by guest on 12 December 2024

Variability. Two subapical antennulary setae called out in Fig. 1C variably ornamented in 3 dissected females: 1 specimen with sparsely spinulated seta and hirsute seta on right antennule (Fig. 1C) and sparsely spinulated seta and naked seta on left antennule (not figured); another specimen with both setae sparsely spinulated on both antennules (not figured); another specimen with both setae naked on both antennules as is typical in other congeners (not figured). One female with 2 apical naked elements on endopod of leg 1 (Fig. 6C) and four plumose setae on second endopodal segment of left leg 3 (Fig. 6D). One male with 1 atrophied seta on third exopodal segment of right leg 3 (Fig. 6E).

Attachment site. Mainly on the head, few on the eyes and body.

Remarks. Examination of the female syntype of *L. longipes* (USNM 12488) from an unknown host and locality, including two specimen lots containing *L. longipes* from GSB captured off La Jolla, California (i.e., Wilson's (1908) 27 female voucher specimens (USNM 38567) and an additional lot (USNM 74301) of five female specimens identified by C. B. Wilson), revealed they are conspecific with our specimens of *Lepeophtheirus* recently collected from GSB off San Onofre, California. Wilson (1905) described and illustrated a 2-segmented abdomen, inwardly curved caudal rami, and a small, curved claw at the tip of a medially concave second endopodal segment of leg 2 in the female, but we did not observe those features in the material noted above. Features of the female of *L. longipes* documented for the first time include the armature of the antennule, the spiniform process on the coxa and ornamentation on the basis of the antenna, the structure of the mandible, the small conical process at the base of the dentiform process of the maxillule, the structure of the maxilla, the ornamentation on the protopod of the maxilliped, the outer spine on the first exopodal segment and accessory process on the middle and inner apical spines on the second exopodal segment of leg 1, the ornamentation on the rami and the proximal outer spine on the third exopodal segment of leg 2, the structure of leg 3, the ornamentation on leg 4, the structure of leg 5, and the armature of the caudal rami.

Examination of Wilson's (1921a) voucher specimens of both sexes of *L. longipes* (USNM 49779) from kelp bass, *Paralabrax clathratus*, captured off Santa Catalina Island revealed they are *Lepeophtheirus constrictus* Wilson, 1908 rather than *L. longipes*. *Lepeophtheirus constrictus* has been previously reported from kelp bass and other related serranids such as spotted sand bass, *Paralabrax maculatofasciatus* (Steindachner, 1868) (type host), and barred sand bass, *Paralabrax nebulifer* (Girard, 1854), captured in waters off southern California (Wilson 1908; Love and Moser 1983). Regardless, a redescription of *L. constrictus* by modern standards is needed.

Examination of specimens of both sexes of *L. longipes* (USNM 180909) from quillback rockfish, *Sebastes maliger*, caught off the San Juan Islands in northwest Washington revealed they are *Lepeophtheirus oblitus* Kabata, 1973 rather than *L. longipes*. Although the collector of those specimens was not provided on the vial label, we are certain they were collected by Nichols (1975), because the collection information provided on the vial label is nearly identical to that in her publication, i.e., "*Udonella caligorum* was found on the parasitic caligoid copepod, *Lepeoptheirus longipes* which infests the skin of the quillback rockfish, *Sebastodes maliger* taken by otter trawl in San Juan Channel (48°35'N, 123°03'W) near Friday Harbor, Washington." *Lepeophtheirus oblitus* also has been reported from quillback rockfish (type host), kelp greenling, *Hexagrammos decagrammus* (Pallas, 1810) (Hexagrammidae Gill, 1889), whitespotted greenling, *Hexagrammos stelleri* Tilesius, 1810, copper rockfish, *Sebastes caurinus* Richardson, 1844, and Pacific ocean perch, *Sebastes alutus* (Gilbert, 1890), captured in waters off western Canada (Kabata 1973, 1988).

Downloaded from http://meridian.allenpress.com/scasbulletin/article-pdf/120/2/64/2930772/i2162-4534-120-2-64.pdf by guest on 12 December 2024

Examination of digital photographs of Brian's (1924) voucher specimens of *L. longipes* from a sharksucker, *Echeneis naucrates*, rubberlip grunt, *Plectorhinchus mediterraneus*, and meagre, *Argyrosomus regius*, captured off Mauritania in northwestern Africa revealed they are not conspecific with *L. longipes*. Furthermore, the two females collected from a meagre and included in the same lot (MNHN-IU-2007-3008 (=MNHN-Cp57)) represent two different species of *Lepeophtheirus*. The female specimen from a sharksucker (Fig. 7A-C) and rubberlip grunt (Fig. 7D-F), as well as one of the two females from a meagre (Fig. 7G-I), differ from the female of *L. longipes* by two or more of the following characters: the genital complex lacks prominent posterolateral lobes; the abdomen is equal in length to the genital complex; the spine on the first exopodal segment of leg 3 is inserted subdistally on the basal swelling; and the inner apical spine on the third exopodal segment of leg 4 is relatively shorter. The other female from a meagre (Fig. 8A-B) differs from the female of *L. longipes* and the other female in the same lot (Fig. 7G-I) by having a genital complex that is about the same length as the cephalothorax, an abdomen that is about two-thirds the length of the cephalothorax, a larger, thinner, and strongly recurved postantennal process, and a sternal furca with widely divergent tines. The male from a meagre (Fig. 8C-D) differs from the male of *L. longipes* by having a shorter third exopodal segment on leg 4 and a shorter inner apical spine on the third exopodal segment of leg 4. We could not determine whether the male from a meagre is conspecific with one of the two females from the same host species based on the limited number of photographs available for this study. To the best of our knowledge, there are no reports of any other nominate species of *Lepeophtheirus* from the sharksucker, rubberlip grunt, and meagre. Since sharksuckers (and other remoras) are known to pick parasites off a wide range of fish taxa (Cressey and Lachner 1970), the female specimen of *Lepeophtheirus* found in the mouth of a sharksucker at the time of capture by T. Monod in 1923 may represent a prey item rather than a parasite association. Suffice it to say, direct observations of Brian's (1924) five specimens of *Lepeophtheirus* are needed to determine their species identity.

L. longipes shares a female genital complex that bears prominent posterolateral lobes and is about half the length of the cephalothorax and just over two times longer than the abdomen with *Lepeophtheirus argentus* Hewitt, 1963, *Lepeophtheirus crassus* (Wilson and Bere, 1936), *Lepeophtheirus formosanus* Ho and Lin, 2010, *Lepeophtheirus heegaardi* Hewitt, 1963, *Lepeophtheirus nordmanni* (Milne-Edwards, 1840), and *Lepeophtheirus polyprioni* Hewitt, 1963. *L. argentus*, *L. heegaardi*, and *L. polyprioni* were all reported from New Zealand waters, but on unrelated hosts: *L. argentus* on the bluenose warehou, *Hyperoglyphe antarctica* (Carmichael, 1819) (as *Hyperoglyphe porosa*) (Centrolophidae Bonaparte, 1846); *L. heegaardi* on the silver scabbardfish, *Lepidopus caudatus* (Euphrasen, 1788) (Trichiuirdae Rafinesque, 1810); and *L. polyprioni* on the hapuku wreckfish, *Polyprion oxygeneios* (Schneider and Forster, 1801), and wreckfish, *Polyprion americanus* (Bloch and Schneider, 1801) (as *Polyprion moeone*) (Polyprionidae) (Hewitt 1963). *Lepeophtheirus crassus* is a widely distributed species that is host specific to remoras (Echeneidae) (Lewis 1967; Ho et al. 2006). *Lepeophtheirus nordmanni* and *L. formosanus* are both host specific to the ocean sunfish, *Mola mola* (Linnaeus, 1758) (Molidae Bonaparte, 1832), but *L. nordmanni* has a cosmopolitan distribution whereas *L. formosanus* has been reported only off Taiwan (Kabata 1979; Ho and Lin 2010).

Lepeophtheirus argentus can be distinguished from *L. longipes* by the larger body size (9.55-11.00 mm vs. 8.10-8.53 mm) and having a suborbicular genital complex, a distinctly 2-segmented abdomen, an antennule without a small conical process on the first segment,

Downloaded from http://meridian.allenpress.com/scasbulletin/article-pdf/120/2/64/2930772/i2162-4534-120-2-64.pdf by guest on 12 December 2024

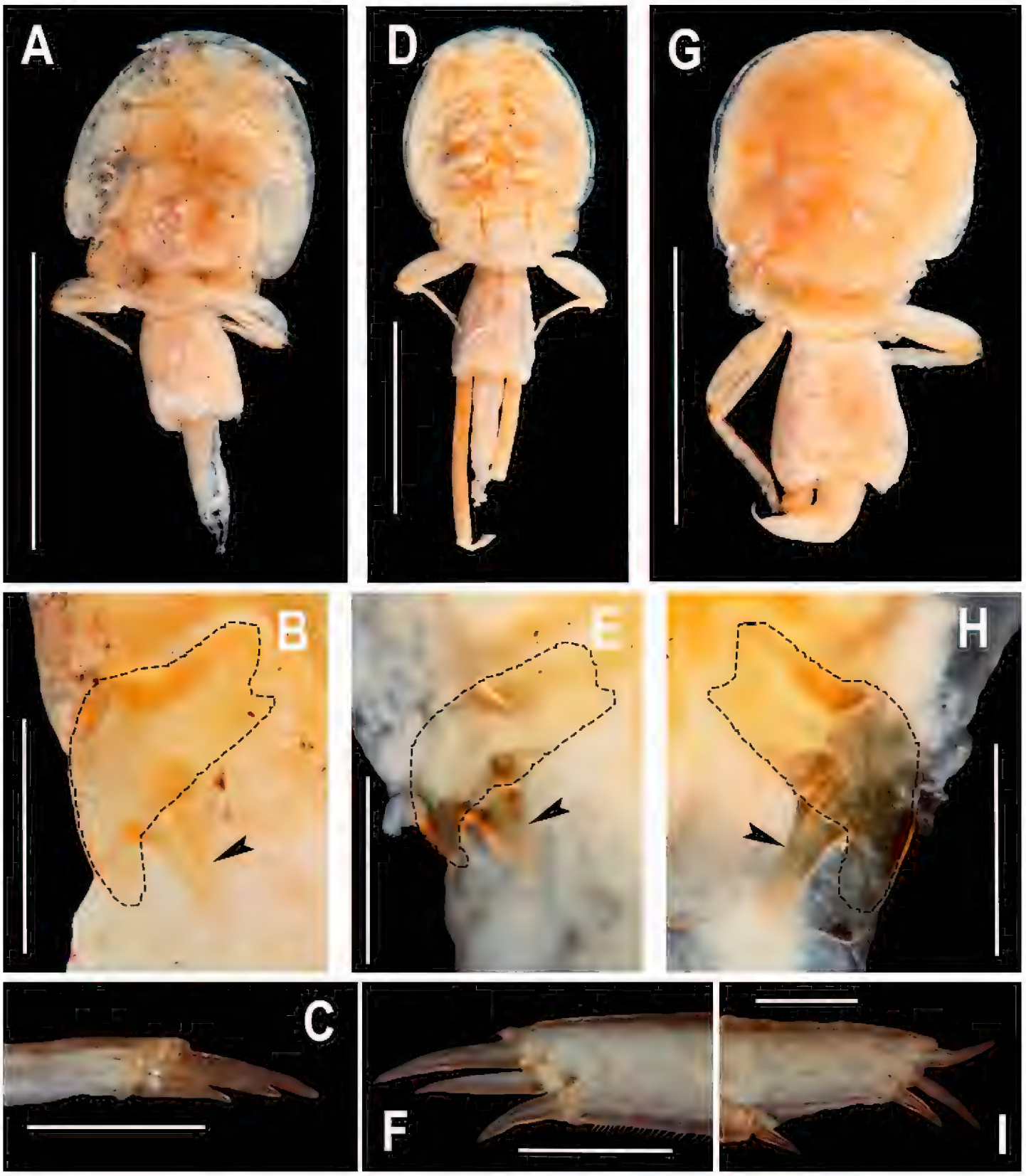

Fig. 7. *Lepeophtheirus* sp., adult female, specimen MNHN-IU-2007-2964 (=MNHN-Cp53) (A-C), specimen MNHN-IU-2007-2975 (=MNHN-Cp54) (D-F), and specimen MNHN-IU-2007-3008 (=MNHN-Cp57) (G-I). A) Habitus, dorsal; B) First exopodal segment of right leg 3, with dashed line indicating segment edge and arrowhead indicating subapical spine, ventral; C) Third exopodal segment of right leg 4, ventral; D) Habitus, ventral; E) First exopodal segment of right leg 3, with dashed line indicating segment edge and arrowhead indicating subapical spine, ventral; F) Third exopodal segment of left leg 4, ventral; G) Habitus, dorsal; H) First exopodal segment of left leg 3, with dashed line indicating segment edge and arrowhead indicating subapical spine, ventral; I) Third exopodal segment of right leg 4, ventral. Scale bars: 5 mm for A, D, G; 0.25 mm for B-C, E-F, H-I. Photos by Sébastien Soubzmaigne (Muséum national d'Histoire naturelle).

Downloaded from http://meridian.allenpress.com/scasbulletin/article-pdf/120/2/64/2930772/i2162-4534-120-2-64.pdf by guest on 12 December 2024

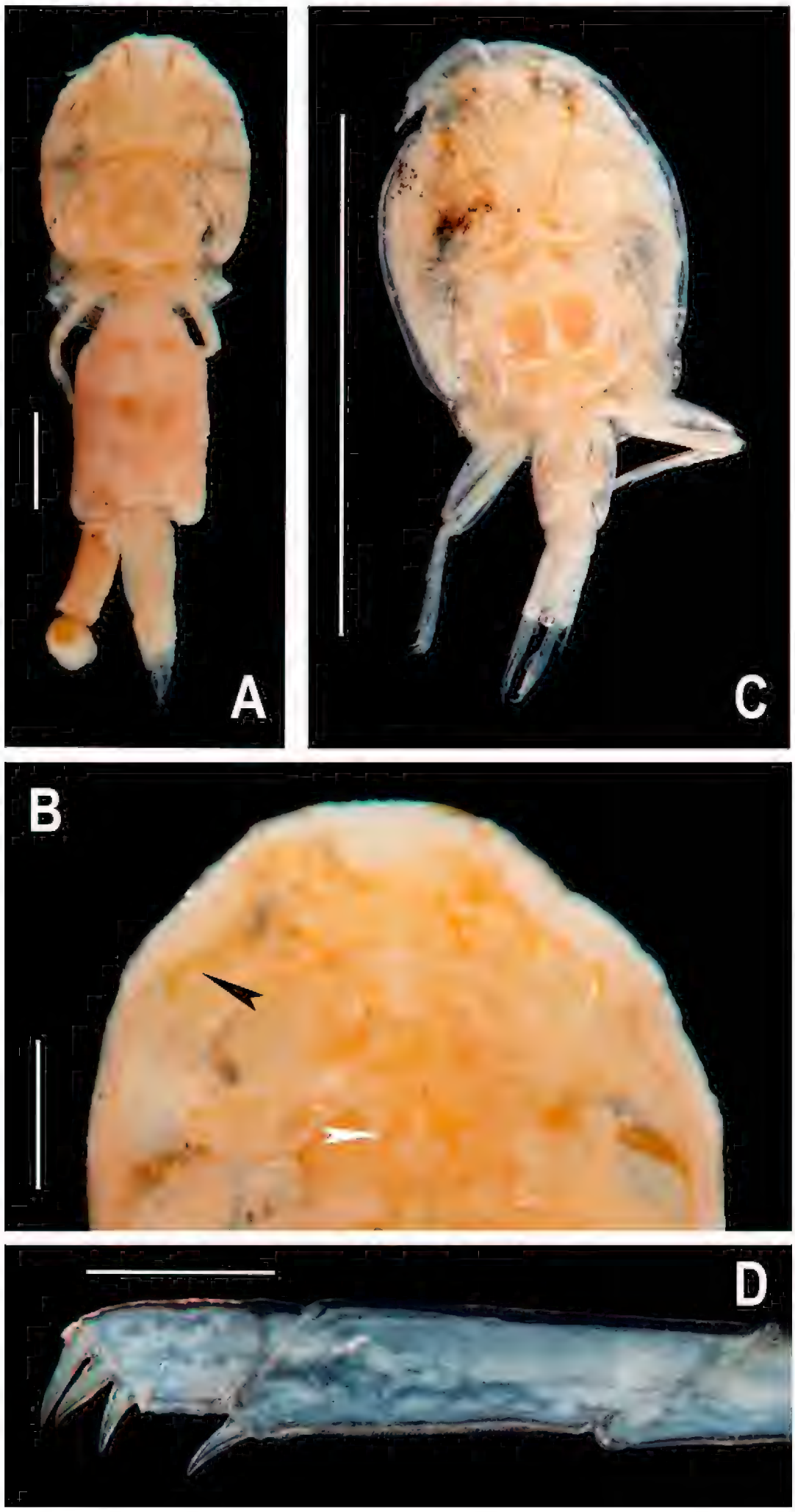

Fig. 8. *Lepeophtheirus* sp., adult female, specimen MNHN-IU-2007-3008 (=MNHN-Cp57) (A-B), and adult male, specimen (MNHN-IU-2007-2986 (=MNHN-Cp55) (C-D). A) Habitus, dorsal; B) Cephalothorax (right postantennal process indicated by black arrowhead; sternal furca indicated by white arrowhead), ventral; C) Habitus, dorsal; D) Exopodal segments of left leg 4, ventral. Scale bars: 1 mm for A-B; 5 mm for C; 0.25 mm for D. Photos by Sébastien Soubzmaigne (Muséum national d'Histoire naturelle).

Downloaded from http://meridian.allenpress.com/scasbulletin/article-pdf/120/2/64/2930772/i2162-4534-120-2-64.pdf by guest on 12 December 2024

a straighter postantennal process, a maxillule with unequal, straight tines and lacking an outer conical process on the dentiform process, an inwardly curved apex on each tine of the sternal furca, a subdistal spine on the first exopodal segment of leg 3, and subequal middle and inner apical spines on the third exopodal segment of leg 4 in the female (Hewitt 1963). In addition, the male of *L. argentus* is larger (6.60-7.00 mm vs. 3.43-3.55 mm) and has a longer first abdominal somite compared to the second abdominal somite, a maxillule that lacks a basal projection on the dentiform process, and apically pointed tines on the sternal furca (Hewitt 1963).

Lepeophtheirus crassus can be delineated from *L. longipes* by the smaller body size (4.56-7.05 mm vs. 8.10-8.53 mm) and having a suborbicular genital complex, a distinctly 2-segmented abdomen, an antennule without a small conical process on the first segment, a blunt process on the antennal coxa, a maxillule lacking an outer conical process on the dentiform process, a sharply pointed apex on each tine of the sternal furca, a shorter second exopodal segment of leg 4, an elongate leg 5 that protrudes beyond the posterolateral process of the genital complex, caudal seta II situated on the outer margin, and a tiny caudal seta VII in the female (Shiino 1960; Lewis 1967). Furthermore, the male of *L. crassus* is slightly larger (4.66-4.80 mm vs. 3.43-3.55 mm) and has a small proximal swelling on the antennal claw, a maxillule that lacks corrugations and a basal projection on the dentiform process, a papilliform protuberance armed with two tiny spinules on the protopod of the maxilliped, apically pointed tines on the sternal furca, and three plumose setae on the free segment of leg 5 (Shiino 1960; Lewis 1967).

Lepeophtheirus formosanus differs from *L. longipes* by having a barrel-shaped abdomen, an antennule lacking a bifid process on the proximal segment, an inner basal accessory process on the postantennal process, a maxillule ornamented with a hyaline membrane on both margins of each tine and lacking a proximal conical process on the dentiform process, an elongate third exopodal segment of leg 3, serrations on the subequal middle and inner apical spines on the third exopodal segment of leg 4, and a triangular leg 5 that is visible in dorsal view in the female (Ho and Lin 2010).

Lepeophtheirus heegaardi can be differentiated from *L. longipes* by having a rounded genital complex, an abdomen that is noticeably wider in the proximal half, an antennule without a small conical process on the first segment, a maxillule lacking an outer conical process on the dentiform process, apically rounded tines on the sternal furca, and subequal middle and inner apical spines on the third exopodal segment of leg 4 in the female (Hewitt 1963).

Lepeophtheirus nordmanni can be distinguished from *L. longipes* by the much larger body size (11.00-12.60 mm vs. 8.10-8.53 mm) and having a blunt process on the coxa and a long, slender claw on the antenna, a slender postantennal process, a maxillule with slender tines and lacking an outer conical process at the base of the dentiform process, slender and apically rounded tines on the sternal furca, a subtriangular process on each side of the sternal furca, a long endopod on leg 1, a long spine on the first exopodal segment of leg 3 that reaches to the second endopodal segment of the same leg, a longer exopod on leg 3, and serrations on the subequal middle and inner apical spines on the third exopodal segment of leg 4 in the female (Shiino 1957; Hewitt 1971; Kabata 1979). Moreover, the male of *L. nordmanni* is larger (6.00-6.90 mm vs. 3.43-3.55 mm) and has a small, subapical secondary process on the antennal claw, a maxillule that lacks corrugations and a basal protuberance on the dentiform process, short tines on the sternal furca, a subtriangular process on each side of the sternal furca, and legs 5 and 6 each represented by a prominent lobe (Hewitt 1971; Kabata 1979).

Downloaded from http://meridian.allenpress.com/scasbulletin/article-pdf/120/2/64/2930772/i2162-4534-120-2-64.pdf by guest on 12 December 2024

Lepeophtheirus polyprioni differs from *L. longipes* by having a rounded genital complex, a distinctly 2-segmented abdomen that is wider proximally, an antennule without a small conical process on the first segment, a maxillule lacking an outer process on the dentiform process, apically rounded tines on the sternal furca, no accessory process on the middle and inner apical spines of the distal exopodal segment of leg 1, and subequal middle and inner apical spines on the third exopodal segment of leg 4 in the female (Hewitt 1963). Additionally, the male is slightly larger (4.20-4.90 mm vs. 3.43-3.55 mm) and has a longer first abdominal somite, an antenna without an accessory process, a maxillule that lacks a basal projection and corrugations on the dentiform process, and a smooth protopod on the maxilliped (Hewitt 1963).

Wilson (1921b) briefly noted that *L. longipes* is closely related to *L. interitus*. *Lepeophtheirus interitus* was established based on a single ovigerous female collected in 1917 from a related polyprionid fish, namely the hapuku wreckfish, *P. oxygeneios* (as *Polyprion prognathus*), captured off the Juan Fernandez Islands, Chile (Wilson 1921b). The hapuku wreckfish was subsequently reported as a host of *L. polyprioni* in New Zealand waters (Hewitt 1963) as noted above. *Lepeophtheirus interitus* has not been reported in the primary literature since its discovery. Wilson (1921b) did not illustrate the inner apical seta, as well as an accessory process on the middle and inner apical spines, on the distal exopodal segment of leg 1 of *L. interitus*, but these features are present in the type material. *Lepeophtheirus interitus* can be distinguished from *L. longipes* by having a smaller body size (5.50 mm vs. 8.10-8.53 mm), a subcircular genital complex that is over three times longer than the abdomen, a maxillule lacking an outer conical process on the dentiform process, and a longer endopod on leg 1 (Wilson 1921b). *Lepeophtheirus interitus* differs from *L. polyprioni* by having a smaller body size (5.50 mm vs. 7.70-8.25 mm), a rectangular 1-segmented abdomen, longer and more widely divergent tines on the sternal furca, and an accessory process on the middle and inner apical spines of the distal exopodal segment of leg 1. Nevertheless, a redescription of *L. interitus* based on fresh specimens from the type host and type locality is needed, since the original description is inadequate by modern standards and the type material accessioned at the Swedish Museum of Natural History, Stockholm, consists of only the maxillule and leg 1 mounted on a slide (Rasmus Hovmöller, pers. comm.).

Discussion

A review of specimens of *Lepeophtheirus* collected from kelp bass captured off Santa Catalina Island (Wilson 1921a), from quillback rockfish caught off the San Juan Islands (Nichols 1975), and from sharksucker, rubberlip grunt, and meagre captured off Mauritania (Brian 1924) revealed they were misidentified as *L. longipes*. In addition, Brian's (1924) female copepod samples from a meagre contained two different species of *Lepeophtheirus*. Rose and Vaissière (1953) and Raibaut et al. (1998) also recorded *L. longipes* on meagre, but from the Mediterranean Sea. Neither record indicated the specific capture location of the host or deposition of voucher material. Both records are doubtful considering the species of *Lepeophtheirus* collected on the same host species from Mauritania are not *L. longipes* as noted above and, more importantly, it is unlikely *L. longipes* occurs in two geographically disparate locations (eastern Pacific and Mediterranean Sea). Hobson's (1971) record of *L. longipes* from treefish from southern California is also doubtful, because *Lepeophtheirus paulus* Cressey, 1969 has been reported from treefish (type host) collected off La Jolla (Cressey 1969), as well as from yellowtail rockfish, *Sebastes flavidus*

Downloaded from http://meridian.allenpress.com/scasbulletin/article-pdf/120/2/64/2930772/i2162-4534-120-2-64.pdf by guest on 12 December 2024

(Ayres, 1862), quillback rockfish, tiger rockfish, *Sebastes nigrocinctus* Ayres, 1859, yelloweye rockfish, *Sebastes ruberrimus* (Cramer, 1895), and walleye pollock, *Gadus chalcogrammus* Pallas, 1814 (as *Theragra chalcogramma*) (Gadidae Rafinesque, 1810) captured in waters off western Canada (Kabata 1973, 1988; Arthur 1984). Collectively, these multiple lines of evidence strongly suggest that *L. longipes* is host specific to GSB. As such, the recent collection of 60 specimens of *L. longipes* from a GSB captured off San Onofre and held at the SCMI represents the first authenticated record of this parasitic copepod in over 100 years. Moreover, this study provides the first description of the male of *L. longipes*.

The life cycle of species of *Lepeophtheirus* consists of eight stages: two naupliar, one copepodid, two chalimi, two pre-adults, and the adult. The naupliar stages are free-swimming, the copepodid is the infective stage, each chalimus stage is attached to a host by a frontal filament, and the pre-adults and adult are mobile over a host's body surface (Venmathi Maran et al. 2013). Semi-transparent caligid copepods of various sizes have been observed on juvenile GSB as small as 7.6 cm in southern California (Fig. 9). Those caligids are likely *L. longipes* based on the high fidelity of this species to GSB as noted above and are probably chalimus, pre-adults, or adult males based on their small size (approximately 1-3 mm) relative to the adult female of *L. longipes* (8.10-8.53 mm). Further research of caligid copepods on juvenile GSB are needed, however, to confirm our hypotheses.

The GSB is a large, charismatic fish, and is thus photographed often by divers. Photographs of adult GSB invariably show large numbers of *L. longipes* attached on the face and a few on the eyes of the host (Fig. 10). The darkly pigmented copepods with a pair of light-colored, cylindrical egg sacs trailing at the posterior end of their body in Fig. 10 are the ovigerous females of *L. longipes*. The thin, white strands hanging off the egg sacs of some females of *L. longipes* in Fig. 10B are individuals of an unidentified species of the hyperparasitic monogenean *Udonella* Johnston, 1835 (Udonellidae Taschenberg, 1879). Fifteen specimens of *L. longipes* in our collection were infected by this unidentified udonellid. Señorita, *Oxyjulis californica* (Günther, 1861) (Labridae Cuvier, 1816), island kelpfish, *Alloclinus holderi* (Lauderbach, 1907) (Labrisomidae Hubbs, 1952), giant kelpfish, *Heterostichus rostratus* Girard, 1854 (Clinidae Swainson, 1839), kelp bass, and bluebanded goby, *Lythrypnus dalli* (Gilbert, 1890) (Gobiidae Cuvier, 1816) have been observed cleaning GSB in California waters (Limbaugh 1955; De Wett-Oleson and Love 2001). The presence of numerous individuals of *L. longipes* often pictured on the head of GSB suggests the grazing success or grazing frequency in the head area of GSB by cleaner fishes is low. While cleaner fishes may be less vulnerable to predation because of the services they provide to predators, they are not entirely immune to being eaten (Hobson 1971).

Acknowledgements

We thank Captain Dennis Dunn and Dennis Mahaffey of the RV Yellowfin, Captain Chris Pica and crew of the MV Reel Fun (Dana Wharf Sportfishing, CA), Captain Mike Abernathy and Kim Anthony of the MV SCE Parker, Jim Cvitanovich, Mike Franklin, Valerie and Tom Handzus, and Danny Warren, all of whom aided greatly in the capture of the giant sea bass specimens. We thank staff at the Southern California Marine Institute for support during parasite collections. We are also grateful to Karen Osborn, Adam Stergis, and Geoff Keel at the Smithsonian Institution, Department of Invertebrate Zoology, Museum Support Center, for kindly arranging the loan of copepod material, Sébastien Soubzmaigne for taking pictures of the specimens of the putative *Lepeophtheirus longipes* deposited at the Muséum national d'Histoire naturelle, Rasmus Hovmöller at the Swedish

Downloaded from http://meridian.allenpress.com/scasbulletin/article-pdf/120/2/64/2930772/i2162-4534-120-2-64.pdf by guest on 12 December 2024

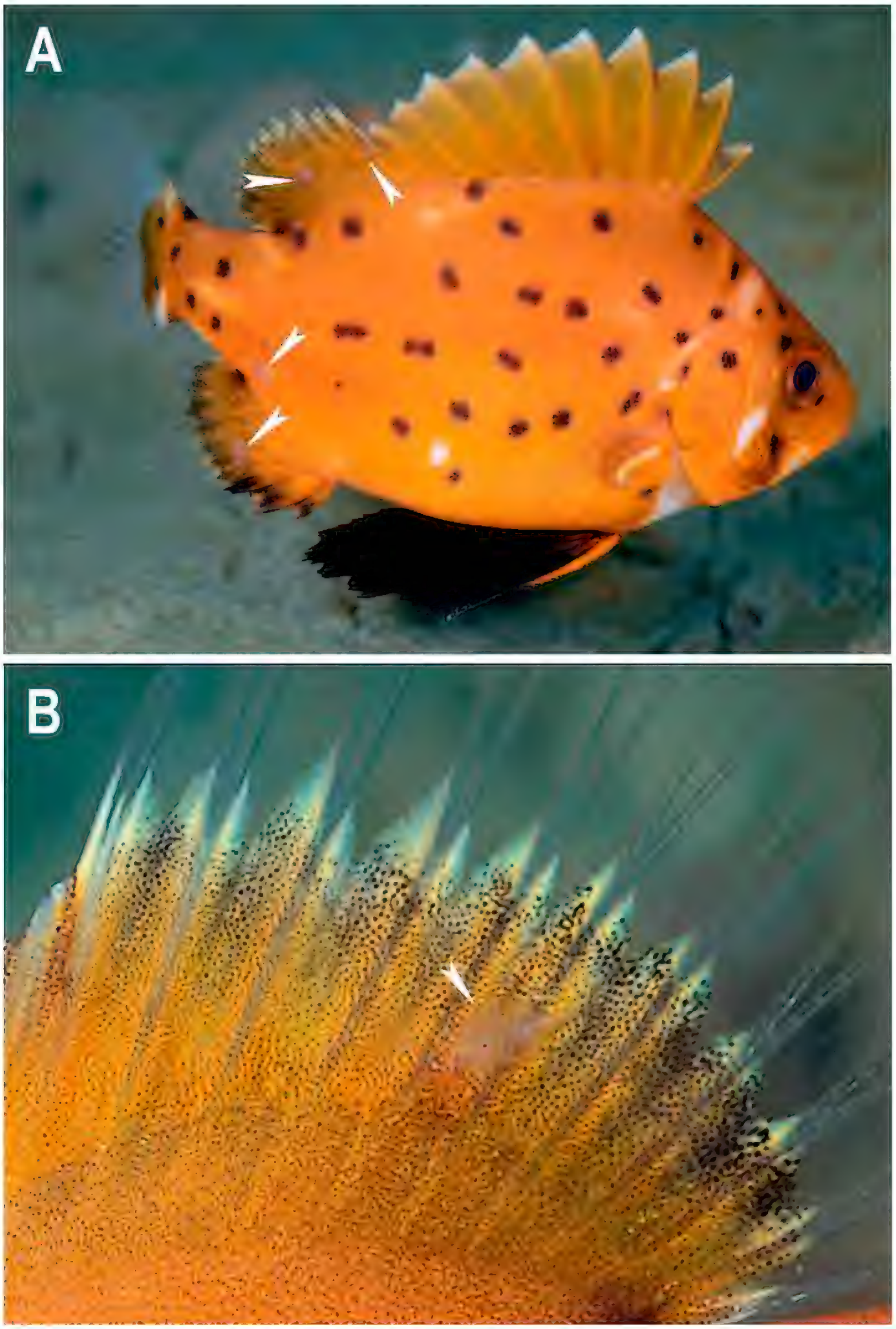

Fig. 9. (A) A juvenile giant sea bass (about 7.6 cm long) with four individuals (indicated by white arrowheads) of an unidentified species of caligid copepod on the right side of its body and fins (photo captured on November 28, 2014 at Newport Pier, California); (B) Close-up image of a caligid copepod (indicated by white arrowhead) on the left side of the soft-rayed portion of the dorsal fin of the same juvenile giant sea bass. Photos by Kevin Lee.

Downloaded from http://meridian.allenpress.com/scasbulletin/article-pdf/120/2/64/2930772/i2162-4534-120-2-64.pdf by guest on 12 December 2024

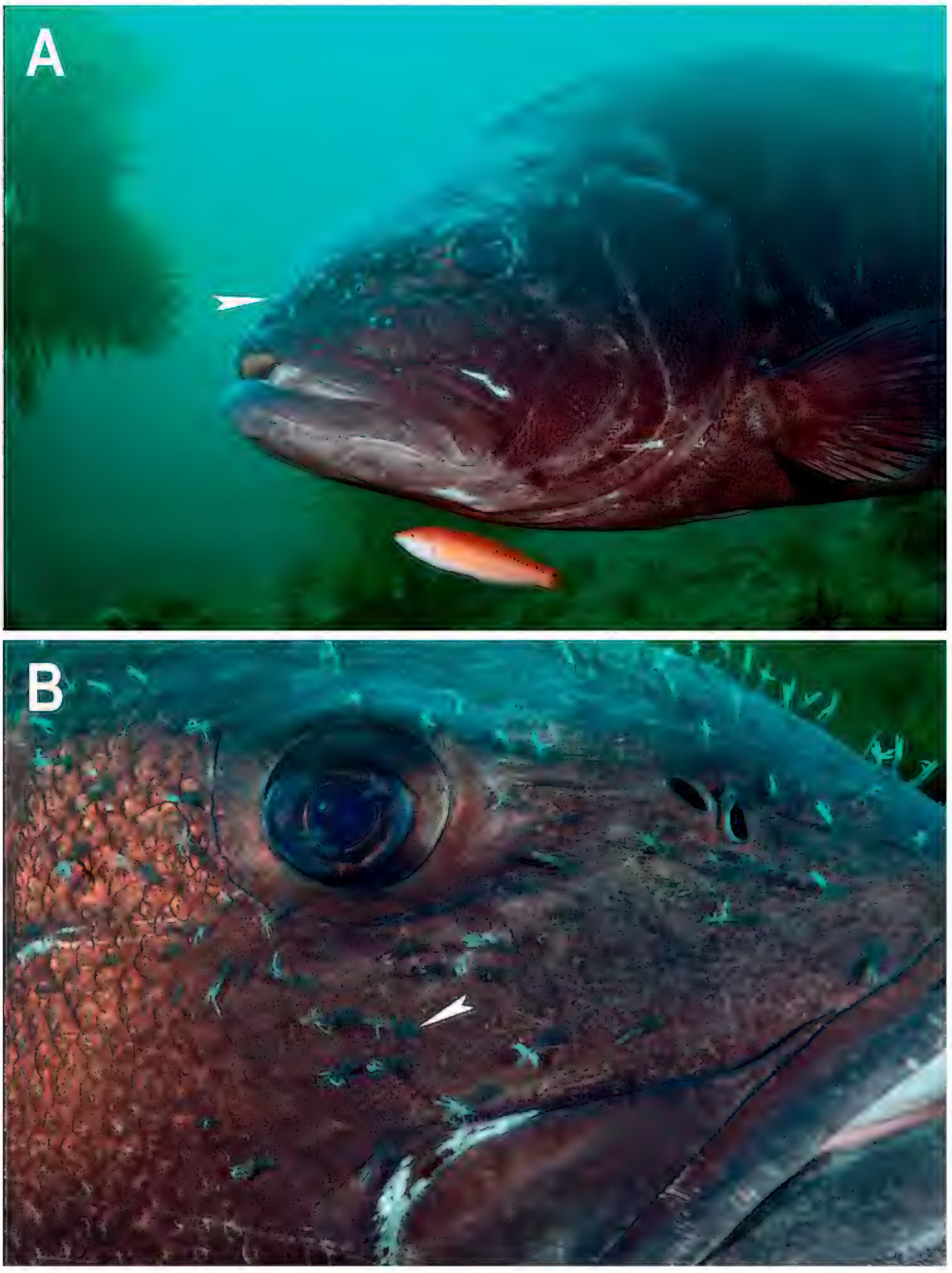

Fig. 10. (A) An adult giant sea bass—flanked below by a rock wrasse, *Halichoeres semicinctus* (Ayres, 1859) (Labridae Cuvier, 1816)—with numerous individuals of *Lepeophtheirus longipes* Wilson, 1905 (one individual indicated by white arrowhead) clustered on its head (photo captured on September 13, 2015 at the Hermosa Artificial Reef, California); (B) Close-up image of individuals of *L. longipes* (one individual indicated by white arrowhead) on the head of the same giant sea bass. Photos by Kevin Lee.

Downloaded from http://meridian.allenpress.com/scasbulletin/article-pdf/120/2/64/2930772/i2162-4534-120-2-64.pdf by guest on 12 December 2024

Museum of Natural History, Stockholm, for providing information on the type material of *Lepeophtheirus interitus*, Kevin Lee for allowing us to use his photos of infected giant sea bass in this study, and Julie O'Donnell for translating pertinent literature.

Literature Cited

Allen, L.G. 2017. GIANTS! Or... The return of the kelp forest king. Copeia, 105:10-13.

—— and A.H. Andrews. 2012. Bomb radiocarbon dating and estimated longevity of giant sea bass (*Stereolepis gigas*). BSCAS, 111:1-14.

Arthur, J.R. 1984. A survey of parasites of walleye pollock (*Theragra chalcogramma*) from the northeastern Pacific Ocean off Canada and a zoogeographical analysis of the parasite fauna of this fish throughout its range. Can. J. Zool., 62:675-684.

Brian, A. 1924. Parasitologia Mauritanica. Matériaux pour la faune parasitologique en Mauritanie. Arthropoda (1re partie). Copepoda. Bull. Com. études hist. sci. Afr. Occident. fr., 1924:365-427.

Chabot, C.L., H.A. Hawk, and L.G. Allen. 2015. Low contemporary effective population size detected in the Critically Endangered giant sea bass, *Stereolepis gigas*, due to fisheries overexploitation. Fish. Res., 172:71-78.

Cornish, A. 2004. *Stereolepis gigas* IUCN 2009. IUCN Red List of Threatened Species, version 2009.1.

Cressey, R.F. 1969. Five new parasitic copepods from California inshore fish. Proc. Biol. Soc. Wash., 82:409-428.

—— and E.A. Lachner. 1970. The parasitic copepod diet and life history of diskfishes (Echeneidae). Copeia, 1970:310-318.

Croker, R.S. 1937. Black sea bass. In: Bureau of Commercial Fisheries. The Commercial Fish Catch of California for the Year 1935. CFG Fish Bull. 49:76-77.

De Wett-Oleson, K. and M. Love. 2001. Observations of cleaning behavior of giant kelpfish, *Heterostichus rostratus*, island kelpfish, *Alloclinus holderi*, bluebanded goby, *Lythrypnus dalli*, and kelp bass, *Paralabrax clathratus*, on giant sea bass, *Stereolepis gigas*. Calif. Fish and Game, 87:87-92.

Dojiri M. and J.-S. Ho. 2013. Systematics of the Caligidae, copepods parasitic on marine fishes. Crustac. Monogr., 18:1-448.

Domeier, M.L. 2001. Giant sea bass. Pp. 209-2121 in California's Marine Living Resources: a Status Report. California Department of Fish and Game.

Froese, R. and D. Pauly (Eds.). 2020. FishBase. World Wide Web electronic publication. Available from http://www.fishbase.org/(accessed 2021).

Hawk, H.A. and L.G. Allen 2014. Age and growth of the giant sea bass, *Stereolepis gigas*. CalCOFI Rep., 55:1-7.

Hewitt, G.C. 1963. Some New Zealand parasitic Copepoda of the family Caligidae. Trans. Royal Soc. New Zeal. Zool., 4:61-115.

——. 1971. Species of *Lepeophtheirus* (Copepoda, Caligidae) recorded from the ocean sunfish (*Mola mola*) and their implications for the caligid genus *Dentigryps*. J. Fish. Res. Board Can., 28: 323-334.

Ho, J.-S. and C.L. Lin. 2010. Three more unrecorded sea lice (Copepoda, Caligidae) parasitic on marine fishes collected off Tai-dong, Taiwan. Crustaceana, 83:1261-1277.

——, B.B. Collette, and I. Madinabeitia. 2006. Host specificity of *Lepeophtheirus crassus* (Wilson and Bere) (Copepoda: Caligidae) parasitic on the marlin sucker *Remora osteochir* (Cuvier) in the Atlantic Ocean. J. Parasitol., 92:1113-1115.

Hobson, E.S. 1971. Cleaning symbiosis among California inshore fishes. Fish. Bull., 69:491-523.

Horn, M.H. and L.A. Ferry-Graham. 2006. Feeding mechanisms and trophic interactions. Pp. 387-410 in The Ecology of Marine Fishes: California and Adjacent Waters. (Allen, L.G., D.J. Pondella II, and M.H. Horn, eds.) Univ. Calif. Press.

House, P.H., B.L.F. Clark, and L.G. Allen. 2016. The return of the king of the kelp forest: distribution, abundance, and biomass of giant sea bass (*Stereolepis gig*as) off Santa Catalina Island, California, 2014-2015. BSCAS, 115:1-14.

Huys, R. and G.A. Boxshall. 1991. Copepod evolution. The Ray Society, 468 pp.

Downloaded from http://meridian.allenpress.com/scasbulletin/article-pdf/120/2/64/2930772/i2162-4534-120-2-64.pdf by guest on 12 December 2024

Kabata, Z. 1973. The species of *Lepeophtheirus* (Copepoda: Caligidae) from fishes of British Columbia. J. Fish. Res. Board Can., 30:729-759.
——. 1979. Parasitic Copepoda of British fishes. The Ray Society, 468 pp.
——. 1988. Copepoda and Branchiura. Pp. 3-127 in Guide to the Parasites of Fishes of Canada. Part II - Crustacea. (L. Margolis and Z. Kabata, eds.) Canadian Special Publication in Fisheries and Aquatic Sciences 101, v+184 pp.
Lewis, A.G. 1967. Copepod crustaceans parasitic on teleost fishes of the Hawaiian Islands. Proc. U. S. Nat. Mus., 121:1-204.
Limbaugh, C. 1955. Fish Life in the Kelp Beds and the Effects of Kelp Harvesting. University of California Institute of Marine Resources, 158 pp.
Love, M.S. and M. Moser. 1983. A Checklist of Parasites of California, Oregon, and Washington Marine and Estuarine Fishes. NOAA Technical Report NMFS SSRF-777, 576 pp.
—— and J.K. Passarelli. 2020. Miller and Lea's Guide to the Coastal Marine Fishes of California. Second Edition. University of California, Agriculture and Natural Resources, California, 418 pp.
Musick, J.A., M.M. Harbin, S.A. Berkeley, G.J. Burgess, A.M. Eklund, L. Findley, R.G. Gilmore, J.T. Golden, D.S. Ha, G.R. Huntsman, J.C. McGovern, S.J. Parker, S.G. Poss, E. Sala, T.W. Schmidt, G.R. Sedberry, H. Weeks, and S.G. Wright. 2000. Marine, estuarine, and diadromous fish stocks at risk of extinction in North America (exclusive of Pacific Salmonids). Fisheries, 25:6-30.
Nichols, K.C. 1975. Observations on lesser-known flatworms: *Udonella*. Int. J. Parasitol., 5:475-482.
Passarelli, J.K. and D. Tang. 2017. A new species of *Lepeophtheirus* (Copepoda; Caligidae) parasitic on three kelpfish species (Clinidae) from the southern California coast. BSCAS, 116:1-16.
Pondella, D.J., II. and L.G. Allen. 2008. The decline and recovery of four predatory fishes from the Southern California Bight. Mar. Biol., 154:307-313.
Raibaut, A., C. Combes, and F. Benoit. 1998. Analysis of the parasitic copepod species richness among Mediterranean fish. J. Mar. Syst., 15:185-206.
Rose, M. and R. Vaissière. 1952. Catalogue préliminaire des Copépodes de l'Afrique du Nord. Bull. Soc. Hist. Nat. Afrique N., 43:113-136.
—— and ——. 1953. Catalogue préliminaire des Copépodes de l'Afrique du Nord (suite III). Bull. Soc. Hist. Nat. Afrique N., 44:83-99.
Shane, M.A., W. Watson, and H.G. Moser. 1996. Polyprionidae: Giant sea basses and wreckfishes. Pp. 873-875 in The Early Stages of Fishes in the California Current Region. (H.G. Moser, ed.) Coop. Fish. Invest. Atlas No. 33. Allen Press Inc.
Shiino, S.M. 1957. Copepods parasitic on Japanese fishes. 13. Parasitic copepods collected off Kesennuma, Miyagi Prefecture. Rep. Fac. Fish. Pref. Univ. Mie, 2:359-375.
——. 1960. Copepods parasitic on remoras from the Bay of Bengal. Rep. Fac. Fish. Pref. Univ. Mie, 3: 542-552.
Venmathi Maran, B.A., S.Y. Moon, S. Ohtsuka, S.-Y. Oh, H.Y. Soh, J.-G. Myoung, A. Iglikowska, and G.A. Boxshall. 2013. The caligid life cycle: new evidence from *Lepeophtheirus elegans* reconciles the cycles of *Caligus* and *Lepeophtheirus* (Copepoda: Caligidae). Parasite, 20:15.
——, E. Suárez-Morales, S. Ohtsuka, H.Y. Soh, and U.W. Hwang. 2016. On the occurrence of caligids (Copepoda: Siphonostomatoida) in the marine plankton: a review and checklist. Zootaxa, 4174: 437-447.
Walter, T.C. and G. Boxshall. 2021. World of Copepods Database. *Lepeophtheirus* von Nordmann, 1832. Accessed through: World Register of Marine Species. Available from http://www.marinespecies.org/copepoda/aphia.php?p=taxdetails&id=13558(accessed March 27, 2021).
Wilson, C.B. 1905. North American parasitic copepods belonging to the family Caligidae, Part I. The Caliginae. Proc. U.S. Nat. Mus., 28:479-672.
——. 1908. North American parasitic copepods: A list of those found upon the fishes of the Pacific coast, with descriptions of new genera and species. Proc. U.S. Nat. Mus., 35:431-481.
——. 1921a. New species and a new genus of parasitic copepods. Proc. U.S. Nat. Mus., 59:1-17.
——. 1921b. Report on the parasitic Copepoda collected during the survey of the Juan Fernandez Islands, 1916-1917. Nat. Hist. Juan Fernandez & Easter Islands, 3:69-74.

Downloaded from http://meridian.allenpress.com/scasbulletin/article-pdf/120/2/64/2930772/i2162-4534-120-2-64.pdf by guest on 12 December 2024

Bull. Southern California Acad. Sci.
120(2), 2021, pp. 88–97
© Southern California Academy of Sciences, 2021

Evaluating the Newly Established Largemouth Blenny (*Labrisomus xanti*) Population off Santa Catalina Island, CA: Determining Densities, Habitat Preference, Size Ranges, and Year Classes

Lindsey N. Stockton, Kathryn C. Scafidi, and Larry G. Allen*

Department of Biology, California State University, Northridge

Abstract.—In 2015 the Pacific Ocean experienced a strong El Niño Southern Oscillation (ENSO). With this change in water temperature, marine species were able to expand outside their previous ranges and settle in new habitats. The first sighting of the species *Labrisomus xanti*, or largemouth blenny, on Santa Catalina Island was October 2015 and since then the species has been seen regularly around the island. In October and November of 2018, we surveyed three sites along the leeward side of Catalina Island. Largemouth blennies were counted, measured, and sex determined along diver transects at multiple depth strata. Substrate type was also recorded. We observed multiple sizes of largemouth blennies among sites, depths and between sexes. Among the three sampled locations, Empire Landing had significantly more individuals than Big Fisherman Cove and Yellowtail Point. These differences were likely due to the greater abundance of small and medium-sized boulders and lack of sand patches within the rocky reef at Empire Landing. Male largemouth blennies were significantly larger than females. The largest largemouth blennies were found at a depth of 4.5 m with the smallest individuals found in the shallow (1.5 m) depths. Individuals were significantly larger at Empire Landing and Yellowtail Point than at Big Fisherman Cove. Finally, length frequency analysis identified at least four putative age classes corresponding to the years 2014–2017 supporting a well-established population. However, further study is necessary before we can determine whether the population at Catalina Island is a self-sustaining population.

Starting in late December 2013, the Northeastern Pacific began to see a warm water mass named "The Blob" (Cavole et al. 2016, Elorriaga-Verplancken et al. 2016). This 2,000 km wide warm water began to expand toward Baja California. By 2015, the Pacific was experiencing a strong El Niño Southern Oscillation (ENSO) (Elorriaga-Verplancken et al. 2016). Southern California began to see unusually warm water. With this change in water temperature, new marine species were able to expand outside their native ranges and settle in new habitats (Cavole et al. 2016, Higgins et al. 2017). Santa Catalina Island, specifically, became home to many new species of fishes (Higgins et al. 2017, Walker et al. 2020).

The first sighting of the species *Labrisomus xanti*, or largemouth blenny, on Santa Catalina Island was October 2015 off Casino Point (Love et al. 2016). The previous known distribution of largemouth blennies ranged from the Pacific coast of Baja California to the southern part of Mexico (Hubbs 1953, Love et al. 2016). Since that first sighting off Casino Point, largemouth blennies have been found at multiple locations around the island, but

* Corresponding author: larry.allen@csun.edu

Downloaded from http://meridian.allenpress.com/scasbulletin/article-pdf/120/2/88/2930763/i2162-4534-120-2-88.pdf by guest on 12 December 2024

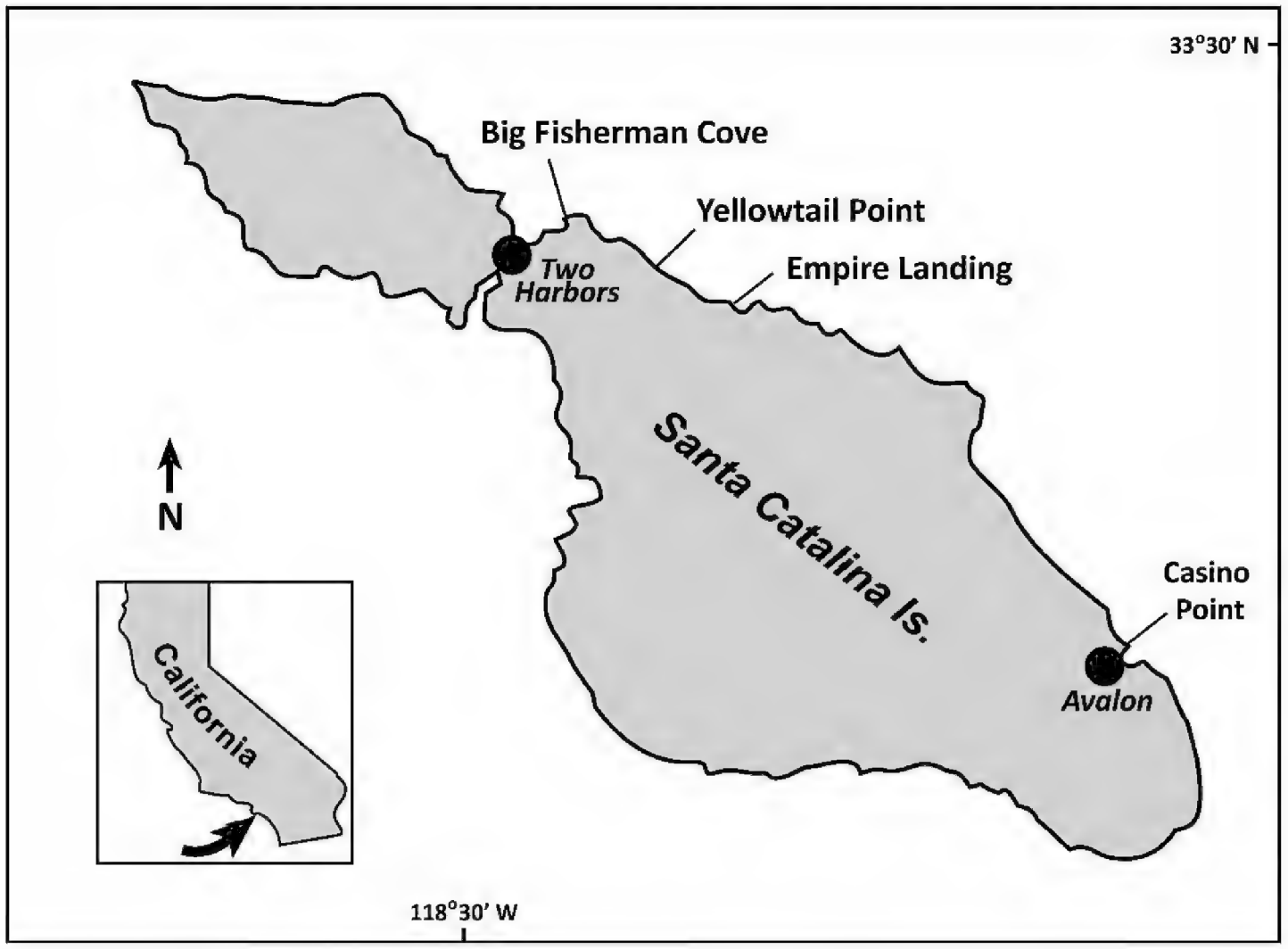

Fig. 1. Location of the three sites surveyed by SCUBA transects dedicated to counting and measuring *Labrisomus xanti* off Santa Catalina Island, CA in October – November 2018.

little has been documented about them. The goals of this project were: 1) to determine what the current densities of *L. xanti* are at three sites along the leeward side of Catalina Island, 2) to distinguish their preferred substrate habitat, and, 3) to determine if this population is made up of multiple size and year classes to examine whether this Catalina Island population is now established.

Materials and Methods

Observations of *L. xanti* were conducted at three sites along the leeward side of Santa Catalina Island, California. The sites were Big Fisherman Cove, Empire Landing, and Yellowtail Point (Fig. 1). Empire Landing and Yellowtail Point were chosen as study sites based on preliminary observations that indicated the presence of *L. xanti.* Big Fisherman Cove was chosen as a study site because it was a leeward location cited in the first published reports of *L. xanti* from California waters (Love et al. 2016). Based on these preliminary observations, largemouth blennies were observed at depths ranging from ~1.5 to 6 m. To execute an accurate survey at each site, observation counts of *L. xanti* were conducted over a 50-meter transect at depths of 1.5 meters, 3 m, 4.5 m, and 6 m. Each transect was completed using SCUBA and all dives were executed within the AAUS Scientific Diving Standards. Divers visually counted largemouth blennies within a 2 m area along the 50 m transect and their sex recorded based on visual coloration.

We also measured each individual and recorded its total length where possible. Size measurements of the largemouth blennies were recorded using a laser measuring device. This

Downloaded from http://meridian.allenpress.com/scasbulletin/article-pdf/120/2/88/2930763/i2162-4534-120-2-88.pdf by guest on 12 December 2024

device consists of two parallel waterproof length-calibrated lasers, set at 25.4 mm apart and paired with a mounted digital video recording GOPRO® (GOPRO, INC. USA) Hero4 camera. The recording of each *L. xanti* were taken at a 90° angle to the video camera with the parallel lasers displayed broadside on the individuals (*cf.* House et al. 2016). Based on a digital image of the largemouth blenny with the 2.54 cm laser reference, we were able to determine the total length of most individuals to the nearest 10 mm. To determine the preferred habitat type of largemouth blennies, we surveyed the substrate of each site using random point contact along each transect. Using a random number generator, 25 points were chosen as the random points to record substrate type along the same 50 m transect after fish counts were conducted. Based on preliminary site observations, the substrate points could be characterized as sand, gravel, cobble (<10 cm), small boulder (10–30 cm), medium boulder (30–100 cm), large boulder (>100 cm) or bench (>100 cm). The transects at four different depths at Big Fisherman Cove, Empire Landing, and Yellowtail Point were conducted three separate times in October and November 2018. Over this time, we conducted 36 transects and habitat type surveys.

Counts of *L. xanti* by site and depth were compared using the statistical platform SYSTAT 13 (Systat Software, Inc.) to run a 2-way Model III ANOVA. A PERMANOVA in the statistical platform R (R package; *vegan*; Oksanen et al. 2018) to compare differences in substrate type among the three sites (Big Fisherman Cove, Empire Landing, and Yellowtail Point). We also created an nMDS plot using R (using the Bray-Curtis Index and square-root transformation) to show the similarities and differences in substrate composition among these sites. The number of blennies per transect was compared to the percent cover of substrate type for each transect using Pearson's Correlation Coefficients calculated in SYSTAT. Sizes (mm TL) of observed largemouth blennies among sexes, sites, and depths were compared using three separate ANOVAs in SYSTAT. When comparing lengths, 14 individuals were omitted because either sex or length could not be measured in the field. These individuals either hid before we could identify their sex or were located within rocks and could not be accurately measured. Male *L. xanti* were distinguished from females based on their coloration. Males exhibit a reddish hue with profuse blue spotting, while females have brown coloring (Love et al. 2016; Fig. 2).

To examine age class structure for *L. xanti*, we used length frequency analysis of the field measured specimens as described in Pauly and David (1981). In this technique, length frequency is plotted in larger class intervals to smooth out small irregularities. A running average is then used to emphasize peaks and intervening troughs. Each frequency value is then divided by the corresponding running average frequency and plotted to identify the most likely center of the age classes represented. Individual fish are then assigned to the corresponding age classes based on size alone. Finally, otoliths from the only two specimens collected off Catalina Island in October 2018 were examined to ground truth the proposed ages based on the length frequency analysis. The otoliths were examined whole (Stepien 1990) and each complete pair of opaque and transparent bands (annuli) were counted as one year.

Results

A total of 73 *L. xanti* were observed among Big Fisherman Cove, Empire Landing, and Yellowtail Point. Empire Landing (Fig. 3) held more individuals n = 39 observed per transect than the other two sites with a significantly higher mean density (No./100 m^2; $F_{[2,33]} = 5.253$, $p = 0.025$, Tukey HSD *post-hoc* test). Twenty-four largemouth blennies were observed at Yellowtail Point and Big Fisherman Cove had the lowest number of individuals

Downloaded from http://meridian.allenpress.com/scasbulletin/article-pdf/120/2/88/2930763/i2162-4534-120-2-88.pdf by guest on 12 December 2024

Fig. 2. Male (left) and female (right) largemouth blennies, *Labrisomus xanti*, exhibiting breeding coloration in their preferred small boulder habitat off Empire Landing, Santa Catalina Island, California, October 2018. Photographs by K. Scafidi.

Downloaded from http://meridian.allenpress.com/scasbulletin/article-pdf/120/2/88/2930763/i2162-4534-120-2-88.pdf by guest on 12 December 2024

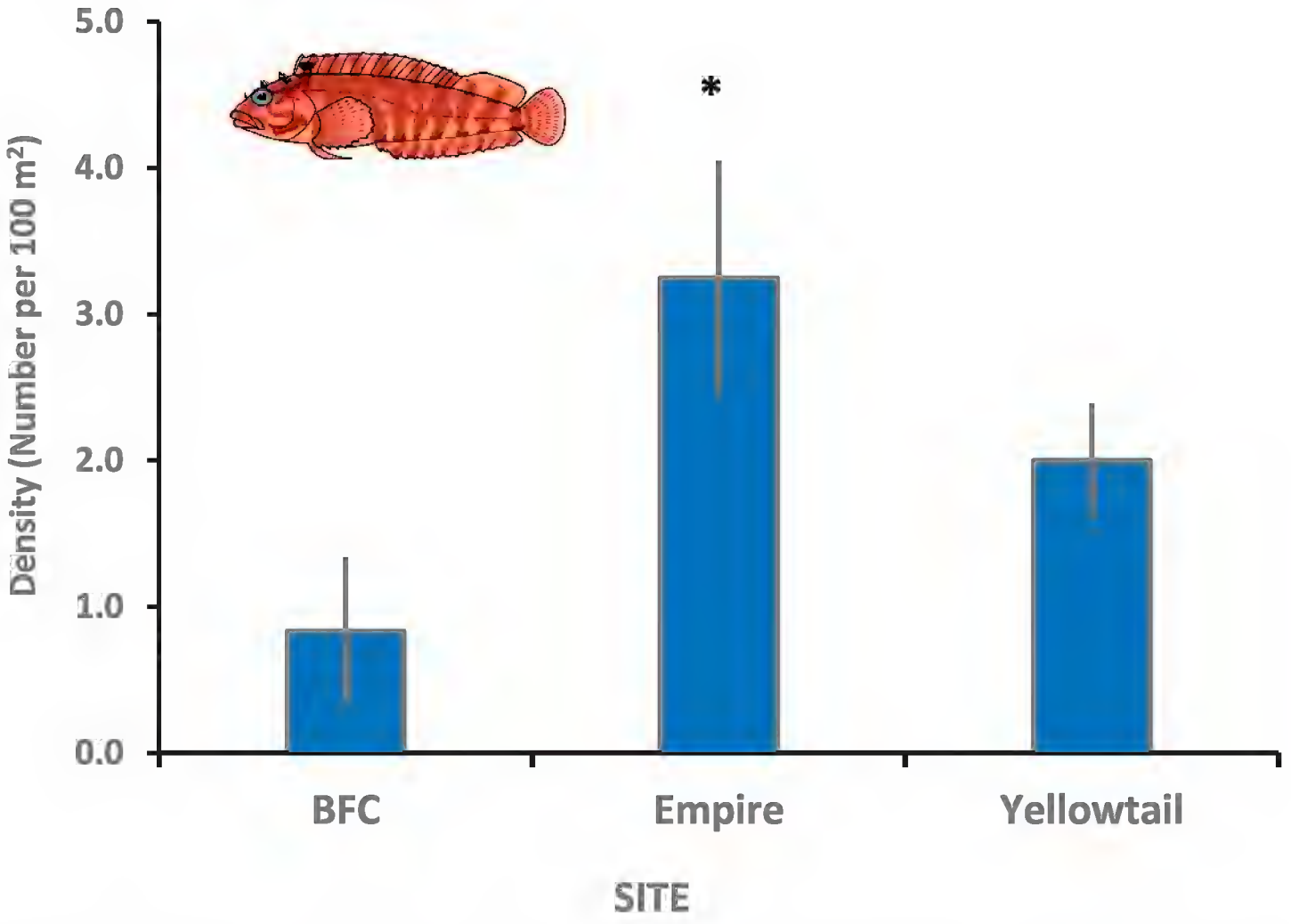

Fig. 3. Mean density (number/100 m^2) of *Labrisomus xanti* by site. (mean +/- SE, $F_{[2,33]} = 5.253$, $P = 0.025$; * - sign. diff. by Tukey HSD *post-hoc* test).

(n = 10). No significant differences in blenny density were found among depths at each site ($F_{[1,3]} = 0.742$, $p = 0.565$). Overall, substrate composition was significantly different among the three sites ($df = 3$, $R^2 = 0.26$, $p < 0.05$) (Fig. 4). Big Fisherman Cove, which had the least number of largemouth blennies, had more sand and cobble with less boulders, while Yellowtail Point and Empire Landing habitats were comprised of mostly small and medium boulders (Fig. 4). We found that the abundance of largemouth blennies was positively correlated with the abundance of small and medium boulders but negatively with the abundance of sandy habitat (Table 1).

Table 1. Correlation coefficients (Pearson *r*) for number of *Labrisomus xanti* versus substrate types ($df = 34$).

Substrate	*r*	
Sand	**−0.355**	*
Gravel	−0.024	
Cobble (<10 cm)	−0.261	
SM Boulder (10-30 cm)	**0.430**	**
Med Boulder (30-100 cm)	**0.278**	*
LG Boulder (>100 cm)	0.122	
Bench (>100 cm)	−0.119	

* - significant at $p < 0.05$ level
** - significant at $p < 0.01$ level

Downloaded from http://meridian.allenpress.com/scasbulletin/article-pdf/120/2/88/2930763/i2162-4534-120-2-88.pdf by guest on 12 December 2024

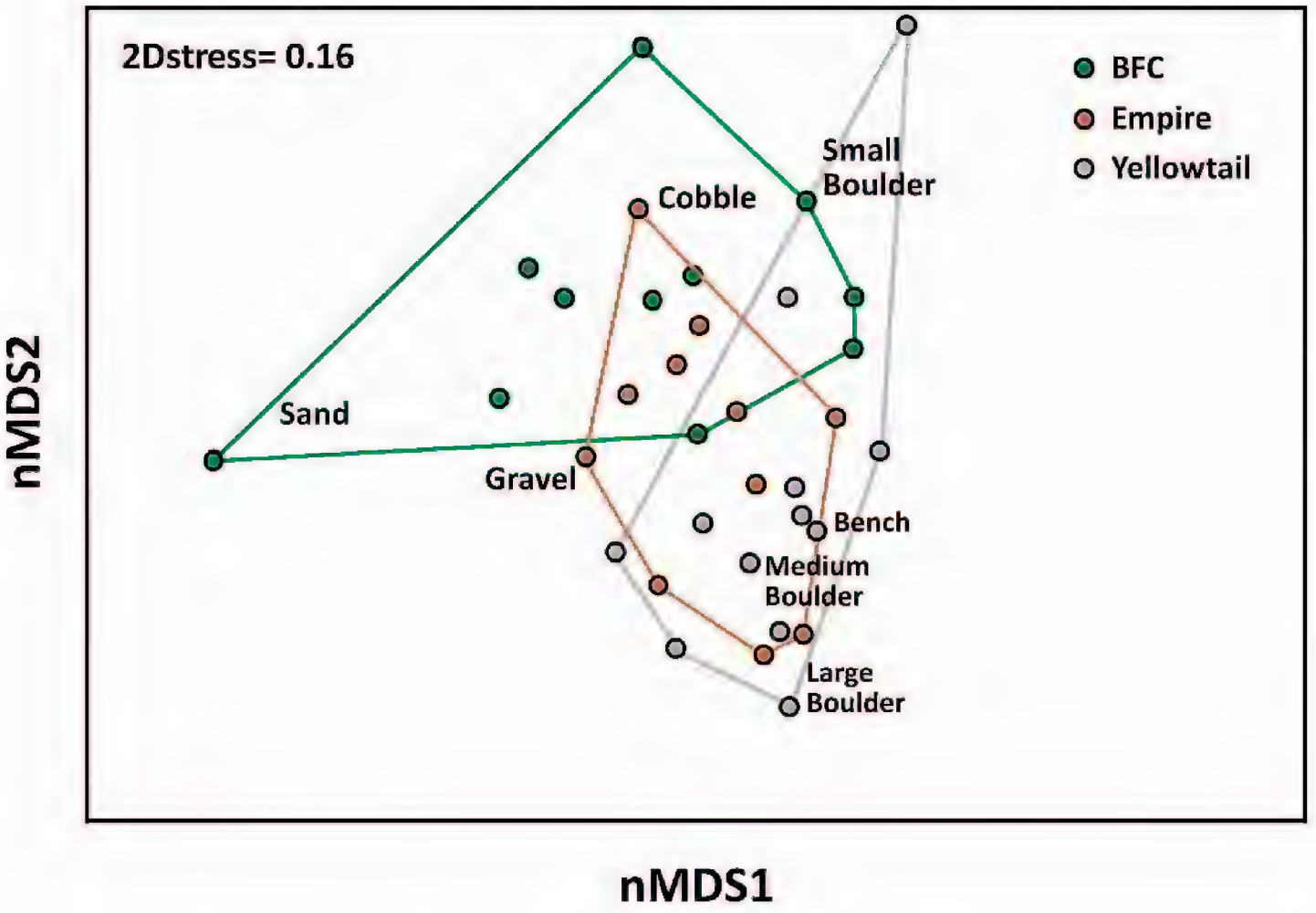

Fig. 4. Comparison of substrate similarities and differences among Big Fisherman Cove (BFC), Empire Landing and Yellowtail Point for *Labrisomus xanti* (PERMANOVA; $R^2 = 0.26$, $p < 0.05$). Each point represents the individual transects at each depth for the three sites. (See Table 1 for description of substrate labels).

The mean total length from all 59 measurements was 138 (± 24 SD) mm TL. Males were significantly larger than females ($F_{[1,57]} = 5.253$, $p = 0.034$) (Fig. 5). The total length of these individuals also varied significantly by depth ranging from 1.5 to 6 m ($F_{[3,55]} = 4.063$, $P = 0.011$*, Tukey HSD *post-hoc* test). The largest *L. xanti* were observed at 3 and 4.5 m, while the smaller *L. xanti* were observed at 1.5 and 6 m. Site was also a significant factor when comparing length of *L. xanti* ($F_{[2,56]} = 5.253$, $P = 0.008$*, Tukey HSD *post-hoc* test). Empire Landing had the largest average individuals and Big Fisherman Cove had the smallest individuals.

Length frequency analysis of the *L. xanti* measured in this study yielded at least four putative year classes (Fig. 6a). We were able to age two individuals collected from the Pin Rock area of Santa Catalina Island in November 2018. Otolith ring counts supported the putative age classes. A 146 mm TL specimen was determined to be 3-years old (2015 year class) while the 131 mm TL blenny was found to be 2-year old (2016 year class). The putative year classes were supported, at least minimally, by otolith ring counts of the two specimens. Number of individuals classified by the recruitment year (Fig. 6b) indicated the establishment of the population at Catalina Island starting in 2014 with solid recruitment in both 2015 and 2016.

Discussion

The 2015 ENSO phenomenon likely played a significant role in tropical species, like the largemouth blenny, expanding their range to Santa Catalina (Love et al. 2016). However,

Downloaded from http://meridian.allenpress.com/scasbulletin/article-pdf/120/2/88/2930763/i2162-4534-120-2-88.pdf by guest on 12 December 2024

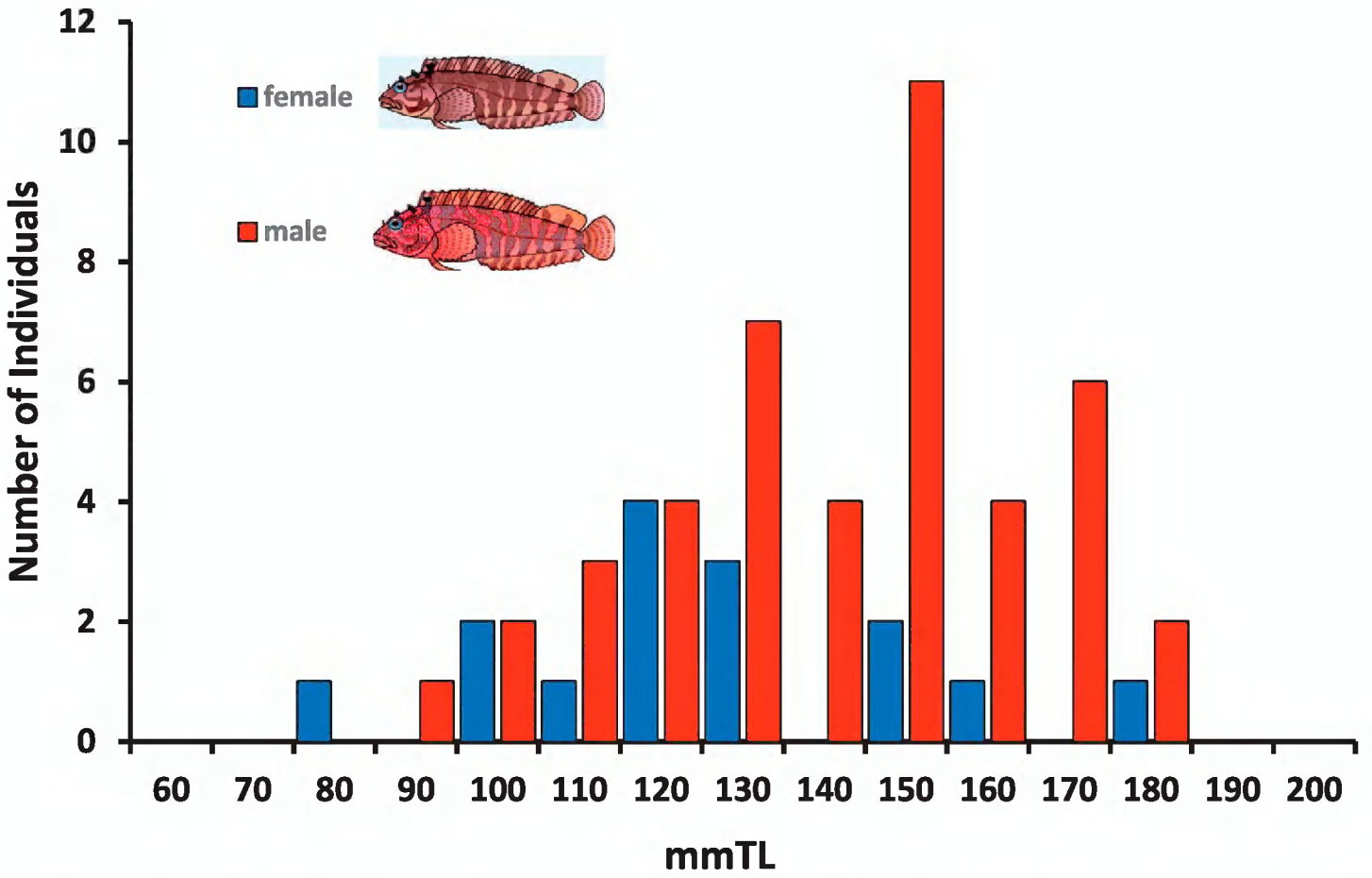

Fig. 5. Comparison of length frequencies (10 mmTL bins) between female and male *Labrisomus xanti* observed over three site at Santa Catalina Island. Males were significantly larger than females overall (mean +/- SE, $F_{[1,57]} = 5.253$, $p = 0.034$*).

prior to this study, little was known about this range expansion event including the current status of the population around Catalina Island. We now know that the *L. xanti* population was relatively abundant in 2018. Among the three sampled locations, Empire Landing had significantly more individuals than Big Fisherman Cove and Yellowtail Point. These differences are likely due to the greater abundance of small and medium sized boulders and lack of sand patches within the rocky reef at Empire Landing.

In order to conclude that a population new to an area was established, evidence of multiple size classes that are the result of consistent year classes was needed. The length frequency analysis documented herein, demonstrates that multiple size classes of *L. xanti* existed among sites, depth strata, and sexes of largemouth blennies. Male largemouth blennies were significantly larger than females. Largemouth blennies were the largest at the 4.5 m depth stratum while the smallest individuals were found in the shallow 1.5 m depths. When comparing sites, we found that largemouth blennies were significantly larger at Empire Landing and Yellowtail Point than Big Fisherman Cove.

Whether these multiple size classes actually correspond to multiple year (age) classes was more difficult to determine because little is known of the age and growth of small, cryptic fish species, especially blennioids, of rocky reef environments in the northeastern Pacific Ocean. We were able to verify the year classes (2015 and 2016) of two individuals from otolith ring counts and total lengths in this study. Stepien (1990) found five year classes represented in the intertidal specimens of another labrisomid, *Auchenionchus microcirrhis*, from Chile based on otolith ring counts. Her findings lend support to our conclusion that *L. xanti,* also a labrisomid, was represented by multiple year classes and could live and persist up to four years in its expanded range to Catalina Island.

Downloaded from http://meridian.allenpress.com/scasbulletin/article-pdf/120/2/88/2930763/i2162-4534-120-2-88.pdf by guest on 12 December 2024

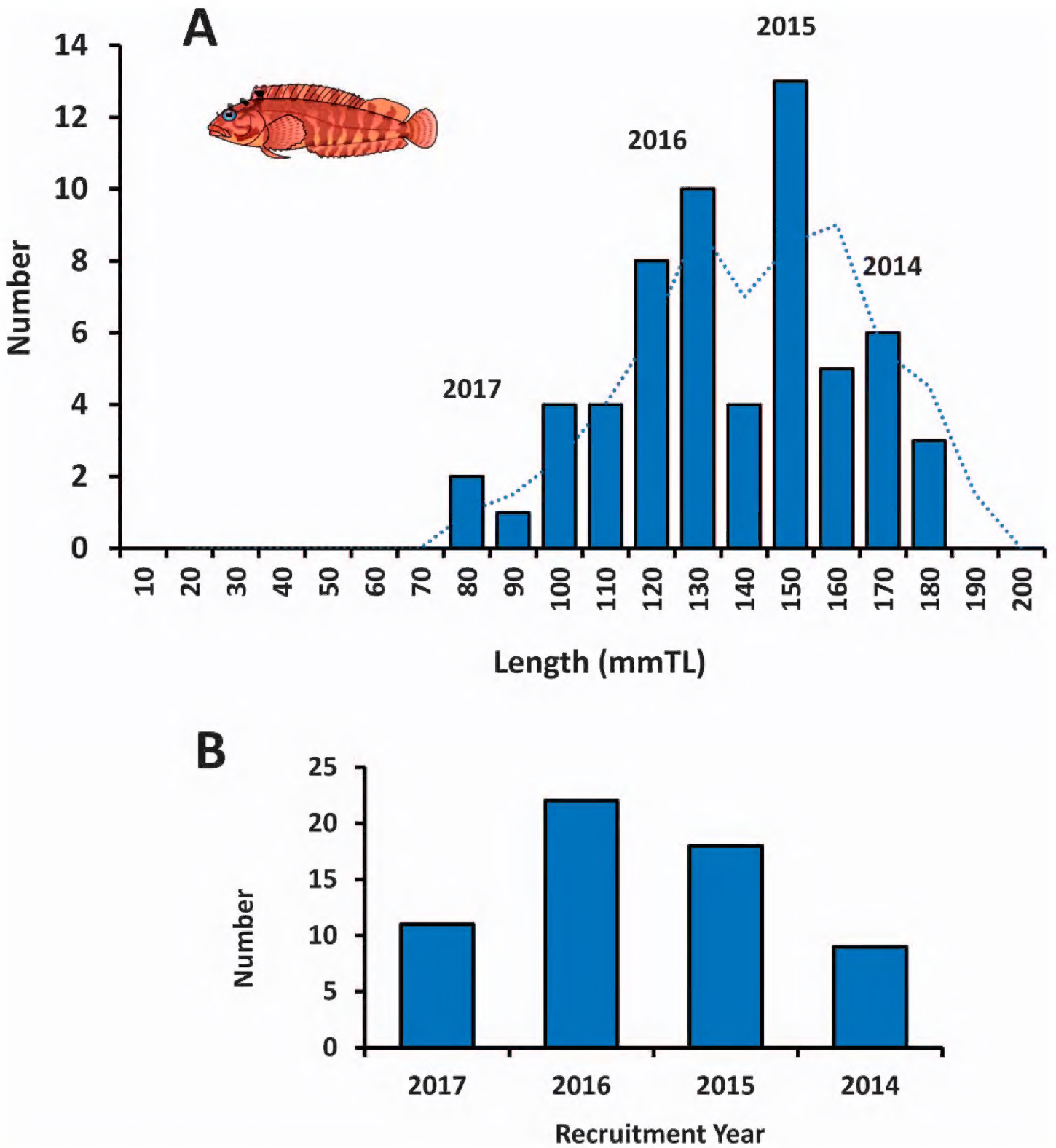

Fig. 6. A) Length frequency of *Labrisomus xanti* measured by 10 mmSL increments. Dotted line traces the two-increment running average of number of individuals per increment. Year labels indicate the estimated recruitment year represented by the peak frequencies. B) Number of individuals classified by recruitment year estimated by length frequency analysis.

If the largemouth blenny population off Catalina Island is well established, is it the result of one or more individual recruitment events? Or are the observed year classes the result of successful reproduction of *L. xanti* around Catalina Island or elsewhere in southern California? Evidence for the successful establishment of southern California reef fish populations based on El Niño events have been documented. Higgins et al. (2017) concluded that El Niño events drive the settlement of recruits of the long-lived California moray (*Gymnothrax mordax*) towards the northern edge of their range off Catalina Island and other Southern California rocky reefs. Likewise, Sturm and Horn (2001) reported similar evidence regarding the establishment of zebraperch (*Kyphosus azureus*) off southern

Downloaded from http://meridian.allenpress.com/scasbulletin/article-pdf/120/2/88/2930763/i2162-4534-120-2-88.pdf by guest on 12 December 2024

California in the 1980s and 1990s. However, evidence for self-sustaining populations once established by a northern range extension are rare. Based on the evidence presented herein, we believe that the population of largemouth blennies off Catalina Island may well be self-sustaining. The initial recruitment events from southern waters were likely related to the warm water years of 2014 (Pacific Warm Anomaly) and 2015 (El Niño). Walker et al. (2020) reported that sea surface temperature (SST) in the Southern California Current System (SCCS) was elevated in the area through at least 2018, including the highest SST ever recorded at Scripps Institute of Oceanography Pier. We found evidence of *L. xanti* year classes from 2016–2017 implying successful recruitment to the island in those years as well. Whether these successful recruits of 2016 and 2017 were produced by the adult fish from Catalina Island or elsewhere in the Southern California Bight (indicating a self-sustaining and established population) or whether they were the result of further larval transport from farther south cannot be determined at this time. Moreover, recent sightings of largemouth blennies (verified by photographs) have been documented by SCUBA divers off Casino Point, Catalina Island during the years of 2019 and 2020, provides added proof of their persistence to date. Obviously, continued studies of the distribution and population genetics of this largemouth blenny population in the SCCS will be necessary in future years before we can conclude that largemouth blennies are truly established.

Acknowledgments

We want to express our gratitude to the following people for making this research possible. Thank you to Mia Adreani and Peter Edmunds for their invaluable input, insight, and review of this research. We are also grateful to Mark Steele and Erika Nava for sharing their preliminary sightings of *L. xanti* in the survey sites. Our utmost gratitude goes to the staff at the USC Wrigley Institute for Environmental Studies for logistical support during surveys. We are also grateful to Dr. Milton Love (UCSB) and two anonymous reviewers for their advice and input to various aspects of this study. This research was supported by funds from the CSUN Department of Biology, Nearshore Marine Fish Research Program (NMFRP), and the CSU Ocean Studies Institute through the support to the CSU Marine Biology Semester, fall 2018. Specimens were collected under the Scientific Collection Permit #00032 issued to L.G. Allen.

Literature Cited

Cavole, L.M., A.M. Demko, R.E. Diner, A. Giddings, I. Koester, C.M.L.S. Pagniello, M.-L. Paulsen, A. Ramirez-Valdez, S.M. Schwenck, N.K. Yen, M.E. Zill, and P.J.S. Franks. 2016. Biological impacts of the 2013–2015 warm-water anomaly in the Northeast Pacific: Winners, losers, and the future. Oceanogr., 29(2):273–285.

Elorriaga-Verplancken, F.R., G.E. Sierra-Rodríguez, H. Rosales-Nanduca, K. Acevedo-Whitehouse, J. Sandoval-Sierra. 2016. Impact of the 2015 El Niño-Southern Oscillation on the abundance and foraging habits of Guadalupe fur seals and California sea lions from the San Benito Archipelago, Mexico. PLOS One, 11(5):0155034.

Higgins, B.A., D. Pearson, and R.S. Mehta, 2017. El Niño episodes coincide with California moray *Gymnothorax mordax* settlement around Santa Catalina Island, California. J. Fish Bio., 90(4):1570-1583.

House, P.H., B.L. Clark, and L.G. Allen 2016. The return of the king of the kelp forest: distribution, abundance, and biomass of giant sea bass (*Stereolepis gigas*) off Santa Catalina Island, California, 2014-2015. BSCAS, 115(1):1-14.

Hubbs, C. (1953). Revision and systematic position of the blenniid fishes of the genus *Neoclinus*. Copeia, 1953(1):11-23.

Downloaded from http://meridian.allenpress.com/scasbulletin/article-pdf/120/2/88/2930763/i2162-4534-120-2-88.pdf by guest on 12 December 2024

Love, M.S., J.K. Passarelli, B. Cantrell and P.A. Hastings. 2016. The largemouth blenny, *Labrisomus xanti*, new to the California marine fauna with a list of and key to the species of *Labrisomidae*, Clinidae, and Chaenopsidae found in California waters. BSCAS, 115(3): 191–197.

Oksanen, J., F. Guillaume Blanchet, M. Friendly, R. Kindt, P. Legendre, D. McGlinn, P.R. Minchin, R.B. O'Hara, G.L. Simpson, P. Solymos, M.H. Stevens, E. Szoecs, and H. Wagner 2020. vegan community ecology package version 2.5-7.

Pauly, D. and N. David. 1981. ELEFAN I, a basic program for the objective extraction of growth parameters form length-frequency data. Berichte der Deutschen Wissenschaftlichen fur Meersforschung, 28(4):205–211.

Santos, R.S., R.D.M. Nash and S.J. Hawkins 1995. Age, growth, and sex ratio of the Azorean rock-pool blenny, *Parablennius sanguinolentus parvicornis*. J. Mar. Biol. Assoc. U.K., 75 (3):751-754.

Stepien, C.A. 1990. Population structure, diets and biogeographic relationships of a rocky intertidal fish assemblage in central Chile: high levels of herbivory in a temperate system. Bull. Mar. Sci., 47(3): 598-612.

Sturm, E.A., and M.H. Horn 2001. Increase in occurrence and abundance of zebraperch (*Hermosilla azurea*) in the Southern California Bight in recent decades. BSCAS, 100(3):170–174.

Walker, H.J., P.A. Hastings, J.R. Hyde, R.N. Lea, O.E. Snodgrass, L.F. Bellquist 2020. Unusual occurrences of fishes in the Southern California Current System during the warm water period of 2014–2018. Estuar. Coast. Shelf Sci., 236:106634.

Downloaded from http://meridian.allenpress.com/scasbulletin/article-pdf/120/2/88/2930763/i2162-4534-120-2-88.pdf by guest on 12 December 2024